e-palli

AMERICAN JOURNAL OF
ENERGY AND NATURAL RESOURCES (AJENR)

ISSN: 2835-9186 (ONLINE)

VOLUME 2 ISSUE 1 (2023)

American Journal of Energy and Natural Resources (AJENR)

Volume 2 Issue 1, Year 2023
ISSN: 2835-9186 (Online)
DOI: https://doi.org/10.54536/ajenr.v2i1.1311
https://journals.e-palli.com/home/index.php/ajenr

Temporal Variability of Solar Energy Availability in the Conditions of the Southern Region of Mozambique

Fernando V. Mucomole[1*], Carlos A. S. Silva[2], Lourenço L. Magaia[3]

Article Information

Received: February 17, 2023

Accepted: March 13, 2023

Published: March 23, 2023

Keywords

Clear Sky Index, Irradiance, Intermediate Sky, Radiation, Variability

ABSTRACT

The use of photovoltaic solar energy is affected by variations in the availability of solar radiation, which creates stability in solar panels. In our case, the need arose to study the temporal variability of solar energy in the southern region of Mozambique. This was followed by a descriptive sequence, applying the analytical method for the classification of days and the analysis of the day's variability of clear, cloudy and intermediate skies in the data from three regional stations. The results show that it was mostly on clear sky days (44.64%), enhancing the use of solar energy. Statistical analysis of the frequency density variability shows that days with intermediate skies have a similar behavior, however they present a smooth decrease, because for variation of clear sky index ΔK_t^* in the interval [-2,2] it is higher. The values of K_t^* vary between 0.3342–1.2764, the minimum is observed in the month of July and the maximum in December and the variations during the daily course of the K^{t*} determined according to its standard deviation show such suitability to the model adopted for the calculation of global irradiation under the clear sky, as an appropriate choice of time interval and amplitude for the study of variations.

INTRODUCTION

The Sun is the closest star to Earth, whose benefits are evident for humanity, its interior is made up of a radiation zone, where fusion reactions take place, the tachocline where it is believed to be the zone where the magnetic fields and the convection zone, in which all hot material is expelled towards the solar surface, and for these reasons it is considered a huge fusion reactor and radiation emitter (Duffie & Beckman, 1991; Greenpro, 2004; Hottel, 1971; Melo, 2003; Perez *et al.*, 2012; Cumbane, 1994; Twidell & Weir, 1996; Zekai, 2008).

When the beam of radiation emitted by the sun enters the earth, it is divided into two components, a direct component (DNI) which is received directly from the sun and a diffuse one (DHI) which is scattered by the atmosphere. The sum of the two radiation components results in global radiation (GHI), and the radiation that reaches earth per surface unit represents solar energy (Duffie & Beckman, 1991; Elsinga & van Sark, 2014; Izidine, 2008; Kumar, 2016; Melo, 2003; Mucomole *et al.*, 2013; Piacentini *et al.*, 2011; Twidell & Weir, 1996; Vianello & Alves, 1991; Mucomole *et al.*, 2021; Zekai, 2008). Therefore, solar energy is intermittent unlike conventional electrical energy generation (e.g., fossil or nuclear) (Perez *et al.*, 2016; Mucomole *et al.*, 2021; Lohmann, 2018). This intermittency (temporal variability) of solar energy is due to various physical phenomena of reduction of its intensity and scattering when it crosses the earth's atmosphere (atmospheric pollution, harmful gases, aerosols, solid particles, atmospheric absorption, scattering, etc.) (Barreto & Pinho, 2008; Devore, 2015; Duffie & Beckman, 1991; Freitas, 2008; Wenham, *et al.*, 2007). Around the world, solar photovoltaics and other renewable energy sources are predicted to represent the effective and ready solution to meet the growing demand for energy and at the same time limit the increasing carbon emissions (EP, 2022; Freitas, 2008; Mucomole *et al.*, 2021; Perez *et al.*, 2012; Twidell & Weir, 1996; Wenham, *et al.*, 2007; Zekai, 2008). Altogether, global solar energy capacity would increase from 480 GW in 2018 to over 8000 GW in 2050, growing the equivalent of almost 9% on average per year (Lohmann, 2018; PER, 2022).

In Mozambique, by the end of 2022, the Electricity of Mozambique (EDM), has announced a total expected solar capacity of 50 MW, with growth expected in the future (EP, 2022; FUNAE, 2012). As a result, the challenges associated with the inherent volatility of photovoltaic energy production and its fundamentals caused by climate-induced heterogeneity, cloud dynamics, pollution, among others, in the field of solar energy could increase considerably (Arias-Castro et.al., 2014; Elsinga & van Sark, 2014; Freitas, 2008; Hoff & Perez, 2010; Hoff & Perez, 2012; Lohmann, *et al.*, 2016; Lohmann, 2018; Liu & Jordan, 1960; Lave & Kleissl, 2010; Lave & Kleissl, 2013; Lave et.al., 2012; Macedo & Fisch, 2017; Perez *et al.*, 2016; Stetz *et al.*, 2015; Twidell & Weir, 1996; Zekai, 2008).

The increase in the variability of solar radiation affects the performance of the output power of a photovoltaic array (creation of hot spots, overloads, disruption, among others) and the reserves of solar batteries sized for standard solar radiation and their location parameters, impacting on the balancing generation, load, maintenance of power quality, frequency and voltage stability this variability can be prolonged for too long, affecting the autonomous or public electrical grid that is injected (Burilo *et al.*, 2012; Calif, R. *et al.*, 2013; Elsinga & van Sark, 2014; Gallego, *et al.*, 2013; Hinkelman, 2013; Luoma *et al.*, 2012; Marcos *et al.*, 2011; Marcos *et al.*, 2011; Mills,

[1] Department of Physics & Energy Research Center, Faculty of Sciences, Eduardo Mondlane University, Mozambique
[2] Department of Mechanical Engineering, Instituto Superior Técnico, University of Lisbon, Portugal
[3] Departmet of Mathematics and Informatics, Faculty of Sciences, Eduardo Mondlane University, Mozambique
[*] Corresponding author's email: fernando.mucomole@uem.mz

2011; Mucomole *et al.*, 2021; Perpiñán, *et al.*, 2009; Perez *et al.*, 2016; Stetz *et al.*, 2015; Van Haaren *et al.*, 2018; Neggers *et al.*, 2003).

In recent studies, the temporal variability, spectra, fluctuations and power output of energy arrays, etc., were evaluated, the applied methods show that the temporal amount of solar radiation for different locations, registers an increase rate and less decrease in days characteristic and non-characteristic (Duffie & Beckman, 1991; Freitas, 2008; Mucomole *et al.*, 2021; Suri *et al.*, 2007; Wenham, *et al.*, 2007; Zekai, 2008; Mucomole *et al.*, 2013).

Such that knowing the dynamics of fluctuations in the temporal variability of solar radiation, through analysis at a lower resolution of about one and ten minutes implemented here, is the key to efficient planning and reliable operation of future electrical networks and their respective subsystems (Arias-Castro *et.al.,* 2014; Barreto & Pinho, 2008; Burilo *et al.*, 2012; Curtright & Apt, 2018; Greenpro, 2004; Hoff & Perez, 2010; Liu & Jordan, 1960; Lave & Kleissl, 2010; Perpiñán, *et al.*, 2009; Perez *et al.*, 2012; Stetz *et al.*, 2015; Twidell & Weir, 1996; Wenham, *et al.*, 2007; Yordanov *et al.*, 2013; Yordanov *et al.*, 2013; Zekai, 2008).

Analysis of the temporal variability of solar radiation, by remote sensing satellite-derived solar radiation data for the region, would also be convenient for analysis of large scales of time intervals. A statistical evaluation of data collected in the years 2020, 2021 and 2022 in the southern region of Mozambique at the convectional station (by pyranometers and pyrheliometers) and at the Davis station (automatic) at the Maputo station of National Institute of Meteorology of Mozambique (INAM), show a margin of error at the margin of 0.5%, smaller, if compared with the satellite data collected at National Oceanic and Atmospheric Administration (NOAH), at the Mapulanguene station which is 0.64%, these differences are combined with the spatial location of the stations, the path of solar radiation, and the frequent reductions it suffers, among others in satellite measurement, in addition to the fact that in most regions there is no record of solar radiation by satellite on a short measurement scale, this dictates the preference for data collected by convectional instruments, the greatest difficulty experienced is that they are time consuming and too expensive to collect, in addition to not being freely accessible (Arias-Castro et.al., 2014; Elsinga & van Sark, 2014; Hottel, 1971; Hoff & Perez, 2010; Hoff & Perez, 2012; Klima. & Apt, 2015; Lohmann, 2018; Liu & Jordan, 1960; Luoma *et al.*, 2012; Madhavan *et al.*, 2016; Marcos *et al.*, 2011; Mills, 2011; Macedo & Fisch, 2017; Ohmura, *et al.*, 1998; Perpiñán, *et al.*, 2009; Piacentini *et al.*, 2011; Perez *et al.*, 2016; Perez *et al.*, 2012; Stetz *et al.*, 2015; Souza, *et al.*, 2005; Twidell & Weir, 1996; Van Haaren *et al.*, 2018; Wenham, *et al.*, 2007; Yordanov *et al.*, 2013; Zekai, 2008).

The southern region of Mozambique is privileged by a high intensity, which has a high climatic potential, which can be used for the production of electricity, agricultural production, poultry, among other projects of interest (Cumbane, 1994; Elsinga & van Sark, 2014; Fernando, 2018; Gallego, *et al.*, 2013; Greenpro, 2004; Hottel, 1971; Hoff & Perez, 2010; Hinkelman, 2013; Inman, *et al.*, 2013; Klima. & Apt, 2015; Lave & Kleissl, 2010; Lonij *et al.*, 2013; Luoma *et al.*, 2012; Madhavan *et al.*, 2016; Melo, 2003; Twidell & Weir, 1996; Vianello & Alves, 1991).

The poor knowledge regarding the temporal variation of this solar resource motivates the determination of the K_t^* index for different years, adopting a time interval of at least one and ten minutes and a period of one day , to evaluate the behavior of the days of the year by classifying the values of the K_t^* index and the standard deviation σK_t^*, to analyze the variability of the global horizontal irradiance for three different types of days of the year, with the main objective of knowing the temporal variability of the availability of solar energy in the southern region of Mozambique, as well as the factors that affect its variability, for better project planning and use of the available solar resource.

MATERIALS AND METHODS

Data Collection and Processing

The sample of solar radiation data (GHI, DNI and DHI) was collected during the measurement campaigns carried out by the Eduardo Mondlane University (UEM) in Maputo (UEM–Maputo station) in 2012, by Mozambique National Energy Fund (FUNAE) in the years 2012, 2013 and 2014 in Maputo in the locality from Lagoa Phati (FUNAE–Maputo–Lagoa Phati station) and in Gaza in the town of Dindiza (FUNAE–Gaza–Dindiza).

(a) **(b)** **(c)**

Figure 1: (a) Pyranometer; (b) Pyranometer with ring and (c) Davis station.

Measurements were made using a PY 5886 pyranometer for data collection of the GHI and DHI solar component (Figure 1. (a) and 1. (b)), a Pyrheliometer which served to collect the DNI component and a Davis station (Figure 1. (c)) installed at the point of higher altitude.

The operational characteristics of Figure 1 are presented in Table 1. A Campbell CR23X data logger was used for data acquisition, operating at a frequency of 1 Hz,

Table 1: Correction factors for types of climates

Sequece	Single sensor species	DNI	GHI
1	Sensor Brand	Pyrheliometer – eppley PY 5886	Pyranometer – epply
2	Calibration Factor	7,9 $\mu V/Wm^{-2}$	7,45 $\mu V/Wm^{-2}$
3	Spectral Range	295-2800 nm	295-2800 nm
4	Response time	1 minut	1 minut
5	Linearity	±0,6%; -a* (0 á 1400 W/m^2)	±0,5% (0 á 1400 W/m^2)
6	Cosine	_____	±1%(0<Z<70°) ±3%(70≤Z<80°)
7	Temperature response	±1% de-22° a+40℃	±1% de-20° a 40℃

storing the instantaneous averages of 1 (one) and 10 (ten) minutes. The data underwent quality control (elimination of spurious values) and were subsequently processed by programs developed specifically for calculating radiation with a time interval of 1 (one) and 10 (ten) minutes.

Sample Size

The sample was prepared in order to perform the calculation with data comprised between the interval during which the sun rises (around 6:00:00 AM) and sets (approximately 6:00:00 PM), thus: in the UEM campaign, at the UEM–Maputo station, the sample obtained comprises only six months of the year 2012, the data only comprise the months of February, March, June, July, November and December, thus comprising a total of 7320 daily data of radiation in the useful area. In the FUNAE campaign, at the FUNAE–Maputo–Lagoon Phati station and at the FUNAE–Gaza–Dindiza station, the sample obtained comprises an interval of three years of full measurement between 2012,2013 and 2014.

The measurement of the three-year project, having started in the fourth month of the year, hence the data only comprise the months of April, May, June, July, August, September, October, November and December, thus comprising a total of about 20367 daily data of radiation in the useful area, in the year 2013 the data comprise all months of the year of full measurement, thus comprising a total of about 27156 daily data of radiation in the useful area and in the year 2014 the data also comprise to all months of the full measurement year, thus comprising a total of about 27156 daily data of radiation in the useful area. For the comparison of the estimation error of measurement of hourly averages, by remote sensing and by convectional instruments, data extracted from NOAAH at the Maputo–Mapulanguene station and those measured at the INAM of Mozambique at the INAM–Maputo station were used, measurements were taken at each station, from the years 2020, 2021 to 2022, each year comprises 12 (twelve) months, thus comprising a total of about 4380 radiation data from the useful area.

Measuring Range

An interval of 1 (one) minute was adopted at the UEM–Maputo station and 10 (ten) minutes for the FUNAE–Maputo–Lagoon Phati station and at the FUNAE–Gaza–Dindiza station. This adopted cadence for a good accuracy of the study in one day is original from the sample of solar radiation data obtained.

GHI spectra and total theoretical radiation as a function of time of day, for an acceptable and non-acceptable day

Due to the intermittency and constant fluctuation of GHI data, for each day of each month of the year, only the range of positive GHI values was taken for the study, as we consider the negative ones to be meaningless for the research. With these data, spectra of GHI and Total Theoretical Radiation were mapped as a function of the time of day, in order to choose an average amount of 10 days with good disposition of radiation for the study, that is, the days where the experimental GHI approaches of total theoretical radiation. For example, a good approximation of a randomly chosen acceptable day was the December 6, 2012, shown in Figure 2 and an unacceptable day was the February 15, 2012 shown in Figure 3, from the UEM–Maputo station.

The analysis using GHI and Total Theoretical Radiation spectra as a function of the time of day showed that the acceptable days for carrying out the research are:

Acceptable days for carrying out the research
UEM–Maputo station
Year 2012

Month of February (analyzed from 1 to 29 days) the 1st, 2nd, 3rd, 4th, 5th, 8th, 9th, 10th, 16th, 18th, 25th, 28th and 29th; Month of March (analyzed from 1 to 31) the 3rd, 4th, 6th, 8th, 10th, 14th, 16th, 17th, 18th, 21st and 28th; Month of June (analyzed from 1 to 30) the 1st, 4th, 5th, 7th, 13th, 27th, 28th and 29th; Month of July (analyzed from 1 to 31 days) the 2nd, 3rd, 4th, 6th, 8th, 10th, 14th, 16th, 17th, 18th, 19th, 22nd and 28th; Month of November (analyzed from 1 to 30 days)

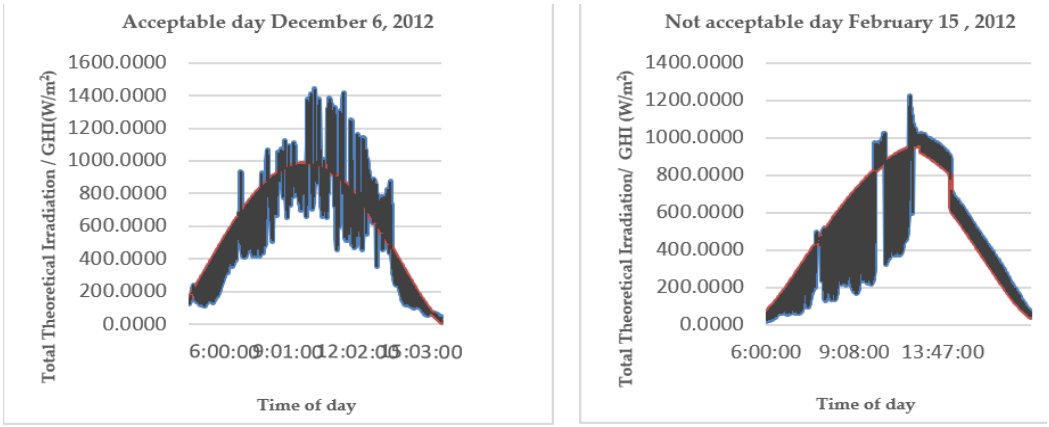

(a) **(b)**

Figure 2: GHI and Total Theoretical Radiation Spectra as a function of Time of Day for (a) Acceptable day (December 6, 2012) and (b) Not acceptable day (February 15, 2012).

the 1st, 2nd, 10th, 11th, 12th, 13th, 15th, 28th and 29th; Month of December (analyzed from 1 to 31 days) the 5th, 6th, 8th, 9th, 10th, 18th, 19th, 20th, 22nd, 23rd, 24th, 25th and 27th.

FUNAE–Gaza–Dindiza station

Year 2012

Month of April (analyzed from 1 to 30 days) the 14th, 15th, 16th and 17th; Month of May (analyzed from 1 to 31 days) the 8th, 12th, 25th and 26th; Month of June (analyzed from 1 to 30 days) the 12th, 23rd, 26th, 27th, 28th and 29th; Month of July (analyzed from 1 to 31 days) the 13th, 17th, 18th, 28th, 29th, 30th and 31st; Month of August (analyzed from 1 to 31 days) the 2nd, 4th, 5th, 8th, 10th, 13th, 15th, 18th, 21st, 22nd, 23rd, 24th, 25th and 31st; Month of September (analyzed from 1 to 30 days) the 3rd, 10th, 12th, 13th, 14th, 18th, 19th, 20th, 21st, 22nd, 24th, 25th, 26th, 27th, 28th and 30th; Month of October (analyzed from 1 to 31 days) the 1st, 2nd, 3rd, 4th, 5th, 6th, 7th, 8th, 9th, 10th, 11th, 14th, 15th, 16th, 18th, 19th, 20th, 22nd, 23rd, 26th, 27th, 28th and 29th; Month of November (analyzed from 1 to 30 days) the 1st, 3rd, 4th, 5th, 6th, 7th, 9th, 11th, 12th, 13th, 14th, 15th, 16th, 17th, 19th, 27th, 29th and 30th; Month of December (analyzed from 1 to 31 days) the 1st, 2nd, 3rd, 5th, 7th, 8th, 9th, 10th, 11th, 12th, 13th, 14th, 15th, 16th, 17th, 18th, 19th, 20th, 21st, 22nd, 23rd, 24th, 25th, 26th, 27th, 28th, 29th, 30th and 31st.

Year 2013

Month of January (analyzed from 1 to 30 days) the 3rd, 6th, 7th, 8th, 9th, 10th, 17th, 18th, 22nd, 23rd, 24th, 25th, 26th, 27th, 28th, 29th, 30th and 31st; Month of February (analyzed from 1 to 28 days) the 1st, 3rd, 4th, 6th, 7th, 8th, 9th, 10th, 11th, 13th, 14th, 15th, 16th, 17th, 18th, 19th, 20th, 21st, 22nd, 23rd, 24th, 25th, 26th, 27th and 28th; Month of March (analyzed from 1 to 31 days) the 1st, 2nd, 6th, 7th, 8th, 9th, 12th, 13th, 14th, 15th, 16th, 17th, 18th, 19th, 20th, 21st, 22nd, 23rd, 24th, 25th, 26th, 27th, 29th, 30th and 31st; Month of April (analyzed from 1 to 30 days) the 2nd, 5th, 6th, 7th, 8th, 9th, 24th, 25th, 26th and 27th; Month of May (analyzed from 1 to 31 days) the 1st, 3rd, 9th, and 15th; Month of June (analyzed from 1 to 30 days) the 7th, 8th, 9th, 13th, 19th, 21st, 22nd, 26th and 30th; Month of July (analyzed from 1 to 30 days) the 7th, 12th, 13th, 14th, 16th, 19th, 20th, and 30th; Month of August (analyzed from 1 to 31 days) the 2nd, 4th, 6th, 13th, 20th, 22nd, 24th, 25th, 26th, 27th and 28th; Month of September (analyzed from 1 to 30 days) the 1st, 2nd, 3rd, 4th, 8th and 9th; Month of October (analyzed from 1 to 31 days) the 1st, 2nd, 3rd, 4th, 5th, 6th, 10th, 11th, 12th, 13th, 15th, 16th, 17th, 18th, 24th, 25th, 26th, 27th, 28th, 29th, 30th and 31st; Month of November (analyzed from 1 to 30 days) the 1st, 4th, 5th, 6th, 7th, 8th, 3th, 14th, 15th, 16th, 17th, 18th, 19th, 20th, 23rd, 24th, 25th, 26th, 27th, 28th, 29th and 30th; Month of December (analyzed from 1 to 31 days) the 1st, 2nd, 3rd, 4th, 5th, 7th, 8th, 9th, 10th, 12th, 14th, 15th, 16th, 20th, 21st, 23rd, 24th and 29th.

Year 2014

Month of January (analyzed from 1 to 31 days) the 1st, 2nd, 3rd, 4th, 10th, 12th, 13th, 15th, 16th, 17th, 19th, 20th, 28th, 29th and 30th; Month of February (analyzed from 1 to 28 days) the 1st, 2nd, 4th, 5th, 6th, 8th, 9th, 10th, 11th, 12th, 14th, 15th, 16th, 18th, 19th, 20th, 23rd, 25th, 27th and 28th; Month of March (analyzed from 1 to 31 days) the 1st, 2nd, 5th, 6th, 7th, 8th, 9th, 12th, 15th, 16th, 17th, 22nd, 23rd, 25th, 26th, 27th, 28th, 29th, 30th and 31st; Month of April (analyzed from 1 to 30 days) the 1st, 2nd, 7th, 9th, 28th; Month of May (analyzed from 1 to 30 days) the 7th, 13th, 17th, 18th, 20th, 27th, and 30th; Month of June (analyzed from 1 to 30 days) the 7th, 8th, 17th, 18th, 20th, 27th and 30th; Month of July (analyzed from 1 to 31 days) the 9th, 15th, 21st, 23rd, 24th, 25th, 30th and 31st; Month of August (analyzed from 1 to 30 days) the 7th, 13th, 14th, 16th, 18th, 23rd, 24th, 25th, 26th, 27th, 30th and 31st; Month of September (analyzed from 1 to 30 days) the 3rd, 4th, 5th, 23rd, 24th, 25th, 26th and 27th; Month of October (analyzed from 1 to 30 days) the 1st, 2nd, 4th, 5th, 6th, 7th, 8th, 9th, 12th, 13th, 14th, 15th, 18th, 19th, 20th, 24th, 28th, 29th and 30th; Month of November (analyzed from 1 to 30 days) the 1st, 2nd, 3rd, 8th, 9th, 10th, 13th, 15th, 18th, 19th, 20th, 21st, 22nd, 23rd, 24th, 25th, 26th, 27th and 28th; Month of December (analyzed from 1 to 30 days) the 3rd, 4th, 5th,

8th, 10th, 11th, 12th, 15th, 18th, 20th, 21st, 22nd, 23rd, 24th, 25th, 26th and 27th.

FUNAE–Maputo–Phati Lagoon Station
Year 2012

Month of April (analyzed from 1 to 31 days) the 27th, 28th, 29th and 30th; Month of May (analyzed from 1 to 31 days) the 7th, 8th, 9th, 12th and 23rd; Month of June (analyzed from 1 to 30 days) the 6th, 15th, 16th, 17th, 18th, 20th, 21st, 22nd, 27th, 28th, 29th and 30th; Month of July (analyzed from 1 to 30 days) the 6th, 16th, 17th, 18th, 20th, 22nd, 28th, 29th, 30th and 31st; Month of August (analyzed from 1 to 31 days) the 8th, 9th, 10th, 11th, 12th and 13th; Month of September (analyzed from 1 to 30 days) the 14th, 15th and 17th.

Search Type and Study Area

This research is descriptive. It is based on the description of the characteristics of a given phenomenon. The collection of experimental data was based on previously described instruments.

The study area is the southern region of Mozambique, which includes the following stations: UEM–Maputo station is located in Maputo City at latitude 25° and longitude 37°; FUNAE–Maputo–Lagoon Phati station, located in Maputo Province, Manhiça district, at 25° latitude and 32° longitude; and the FUNAE–Maputo–Dindiza station, located in the province of Gaza at latitude 25° and longitude 34°, as shown in Figure 3.

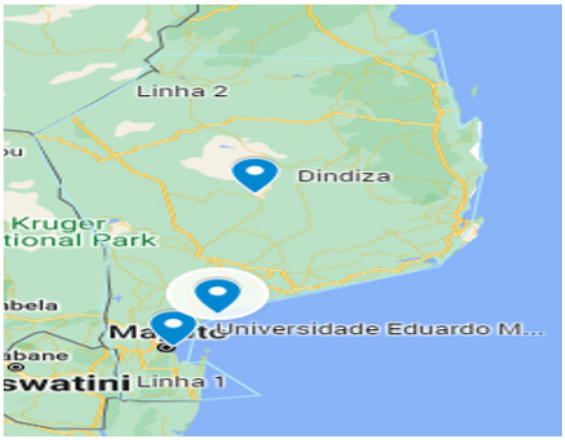

Figure 3: Study area and data collection.

In the sample of data from all stations, some months show fluctuations, as they have missing data for the whole day, or missing for a period of half a day sample

Months Fluctuations of Data Smple
UEM–Maputo Station
Year 2012

In February – for unknown reasons, there were no measurements on the 12th, 13th, 22nd and 23rd; however, there were also half measurements on days 6th (from 10:51:00 AM to 12:36:00 PM), 14th (from 11:06:00 AM to 06:00:00 PM), 24th (01:15:00 PM to 06:00:00 PM) and 27th (9:07:00 AM to 06:00:00 PM); in March – for unknown reasons, there were no measurements on the 23rd, 24th and 25th; however, you also hear half measurements on days 2 (04:29:00 PM to 06:00:00 PM), 5th (12:12:00 PM to 06:00:00 PM), 9th (02:57:00 PM to 06:00:00 PM), 12th (there was "outage of electricity all day" and no measurements were taken), 13th (there was "power return at 9:57:00 AM and failure in the direct radiation cable (cut), the failure was resolved at 12:55:00PM" 09:57:00 AM to 06:00:00 PM), 15th (10:40:00 AM to 06:00:00 PM), 19th (the "Data log with full memory" 8:48:00 AM to 05:45:00 PM), 20th (9:28:00 AM to 06:00:00 PM), 26th (09:01:00 AM to 06:00:00 PM); in the month of June – it was the month with the least drop, having been verified for unknown reasons, that there were no measurements on the 19th, 20th, 21st, 22nd, 23rd, 24th, 25th and 30th; however, you also hear half measurements on days 1st (08:21:00 AM to 06:00:00 PM), 18th (06:00:00 AM to 07:42:00 PM) and 26th (11:56:00 AM to 06:00:00 PM); in the month of July – for unknown reasons, there were no measurements on the 1st, 23rd, 24th and 25th; however, he also hears half measurements on days 5th (12:12:00 PM to 06:00:00 PM), 9th (14:57:00 PM to 06:00 PM), 12th (here "no data due to lack of current all day"), 13th ("power return at 09:57:00 AM and failure in the direct radiation cable (cut), failure resolved at 12:55:00 PM" 09:57:00 AM to 06:00:00 PM), 15th (10:40:00 AM to 06:00 PM), 30th (10:38:00 AM to 18:00 PM); in November – for unknown reasons, there were no measurements on the 4th, 5th, 6th, 7th, 17th, 18th, 19th, 20th, 21st, 22nd, 23rd, 24th, 25th and 30th; however, you also hear half measurements on days 3rd (6:00:00 AM to 13:20:00 PM), 8th (12:40 PM to 18:00 PM), 16th (6:00:00 AM to 02:15:00 PM), 26th (10:57:00 AM to 06:00:00 PM), 27th (06:00:00 AM to 06:00:00 PM) and in the month of December – for unknown reasons, there were no measurements on days 1st, 2nd, 12th, 13th, 14th, 15th, 16th, 28th, 29th and 30th; but also hear half measurements on days 3rd (02:21 PM to 06:00 AM), 7th (06:00 AM to 02:07:07 PM), 11th (10:25:00 AM to 06:00:00 PM), 17th (11:20:00 AM at 06:00:00 PM), 26th (06:00:00 AM to 05:00:00 PM), 31st (09:54:00 AM to 06:00:00PM).

FUNAE–Gaza–Dindiza Station
Year 2012

In April – due to the fact that the measurement project started this year at this station, there were no measurements on the 1st, 2nd, 3rd, 4th, 5th, 7th, 8th, 9th, 10th, 11th and 12th; there was no data collection on day 6th, with only two values falling in the interval from 07:00:00 AM to 07:10:00 AM; on the 15th, 16th, 17th, 18th, 19th, 20th, 21st, 22nd, 23rd, 24th, 25th, 26th, 27th, 28th, 29th and 30th the system only downloaded values equal to zero in the interval from 5:40:00 PM to 06:00:00 PM hours; in the month of May – on the 1st, 2nd, 3rd, 4th, 5th, 6th, 7th, 8th and 9th, the system only downloaded values equal to zero in the interval from 5:30:00 PM to 6:00:00 PM; on 10th, 11th, 12th, 13th, 14th, 15th, 16th, 17th, 18th, 19th, 20th, 21st, 22nd, 23rd, 24th, 25th, 26th, 29th, 30th and 31st days the system only downloaded values equal to zero in the interval from 5:20 PM to 6:00:00 PM and on the 27th, the system only downloaded values equal

to zero in the interval from 5:10:00 PM to 6:00 PM; in the month of June – on the 1st, 2nd, 3rd, 4th, 5th, 6th, 7th, 8th, 9th, 10th, 12th, 13th, 14th, 16th, 17th, 18th, 20th, 22nd, 23rd, 26th, 27th, 28th and 30th the system only downloaded values equal to zero between 6:00:00 AM and 5:20:00 PM to 6:00:00 PM; on the 15th and 19th, the system only downloaded values equal to zero between 6:00:00 AM and 5:10:00 PM to 6:00 PM; on the 21st, 24th, 25th and 28th, the system only downloaded values equal to zero in the interval from 6:00:00 AM to 6:00:00 AM and from 5:20:00 PM to 6:00:00 PM; in the month of July – on the 1st, 2nd, 3rd, 4th, 5th, 8th, 9th, 10th, 13th and 14th the system only downloaded values equal to zero in the interval from 6:00:00 AM to 6:10:00 AM and beyond from 5:20:00 PM to 6:00:00 PM; on the 5th, 6th and 12th the system only downloaded values equal to zero in the interval from 6:00:00 AM to 6:20:00 AM and from 5:20:00 PM to 6:00:00 PM; on the 15th, 16th, 17th, 18th, 19th, 20th, 21st, 22nd, 23rd, 24th, 25th, 26th, 27th, 28th, 29th, 30th and 31st the system only downloaded values equal to zero in the interval of 6:00:00 AM to 6:10:00 AM and from 5:30:00 PM to 6:00:00 PM;

In the month of August – on days 1st, 2nd and 5th the system only downloaded values equal to zero in the interval from 06:00:00 AM to 06:10:00 Am and from 17:30:00 PM to 18:00:00 PM; on the 3rd, 9th, 10th, 11th, 12th, 13th, 14th, 16th, 17th, 18th, 19th, 20th, 21st, 22nd, 23rd, 24th, 25th, 26th, 27th, 28th and 29th, the system only downloaded amounts equal to the zero in the interval from 5:40:00 PM to 6:00:00 PM; on the 4th, 7th, 8th, 9th and 15th the system only downloaded values equal to zero in the interval from 6:00:00 AM to 6:10:00 AM and from 5:40:00 PM to 6:00:00 PM ; on the 6th, the system only downloaded values equal to zero in the interval from 5:30:00 PM to 6:00:00 PM; on the 30th and 31st the system only downloaded values equal to zero in the interval from 5:50:00 PM to 6:00:00 PM; in the month of September – on the 1st, 2nd, 4th, 6th, 7th, 9th and 29th, the system only downloaded values equal to zero in the interval from 5:40:00 PM to 6:00:00 PM; on days 3rd, 10th, 11th, 12th, 14th, 17th, 18th, 19th, 20th, 21st, 22nd, 23rd, 24th, 25th, 26th, 27th and 28th the system only downloaded values equal to zero in the interval from 5:20:00 PM to 6:00:00 PM;

On the 15th and 16th the system only downloaded values equal to zero in the interval from 5:30 PM to 6:00 PM; in October – on days 1st, 2nd, 3rd, 4th, 5th, 6th, 7th, 8th, 9th, 10th, 11th, 12th, 16th, 17th, 18th, 19th, 20th, 21st, 22nd, 23rd, 24th, 25th, 26th, 27th and 30th the system only downloaded values equal to zero in the interval from 5:50 PM to 6:00:00 PM; on the 10th, 11th, 17th, 20th and 24th the system only downloaded values equal to zero in the interval from 5:40 PM to 6:00:00 PM; on the 12th, the system only downloaded values equal to zero in the interval from 5:20:00 PM to 6:00:00 PM; on the 23rd, the system only downloaded values equal to zero in the interval from 5:30:00 PM to 6:00:00 PM; in November – on the 1st, 2nd, 3rd, 4th, 5th, 11th, 12th, 13th, 14th, 15th, 16th, 17th, 18th, 19th, 20th, 21st, 24th, 26th, 27th, 28th, 29th and 30th system downloaded all data fluently (interval from 6:00:00 AM to 6:00:00 AM); on the 6th, 22nd and 23rd the system only measured data in the interval from 6:00:00 AM to 11:50:00 AM, and did not register measurements for the rest of the day; on the 8th, the system was measuring data only in the interval from 6:00:00 AM to 11:20:00 AM, and did not register measurements for the rest of the day; on the 7th, the system was measuring data only in the interval from 6:00:00 AM to 12:20:00 AM, and did not register measurements for the rest of the day; on the 9th, 10th and 25th the system only downloaded values equal to zero in the interval from 17:50:00 PM to 18:00:00 PM and in the month of December – during all days of the month, the system fluently downloaded all data (range from 6:00:00 AM to 6:00:00 PM).

Year 2013

In the month of January – on the 15th, the system only downloaded values equal to zero in the interval from 3:40:00 PM to 6:00:00 PM; the system downloaded all data fluently on days 1st, 2nd, 3rd, 4th, 5th, 6th, 7th, 8th, 9th, 10th, 11th, 12th, 16th, 17th, 18th, 19th, 20th, 21st, 22nd, 23rd, 24th, 25th, 26th, 27th, 28th, 29th, 30th and 31st in the interval from 6:00:00 AM to 6:00:00 PM; in February – the system downloaded all data fluently on all days of the month (that is, from the 1st to the 28th) in the interval from 06:00:00 AM to 06:00:00 PM; in March – the system downloaded all data fluently on days 1st, 2nd, 3rd, 4th, 5th, 6th, 7th, 8th, 9th, 10th, 11th, 12th, 16th, 17th, 18th, 19th, 20th, 21st, 22nd and 23rd in the interval from 6:00:00 AM to 6:00:00 PM;

On the 24th, 25th, 26th, 27th, 28th and 30th the system only downloaded values equal to zero in the interval from 5:50:00 PM to 6:00:00 PM; on the 29th and 31st the system only downloaded values equal to zero in the interval from 5:40:00 PM to 6:00:00 PM; in the month of April – on the 1st, 2nd, 5th, 6th, 7th, 8th and 9th the system only downloaded values equal to zero in the interval from 5:40:00 PM to 6:00:00 PM; on the 3rd, 4th, 10th, 12th, 13th, 14th, 15th, 16th, 17th, 18th, 19th and 22nd the system only downloaded values equal to zero in the interval from 5:30:00 PM to 6:00:00 PM; on the 11th, 20th, 21st, 24th, 25th, 26th, 27th, 28th, 29th and 30th the system only downloaded values equal to zero in the interval from 5:20:00 PM to 6:00:00 PM;

In the month of May – on the 1st, 2nd, 3rd, 4th, 5th, 6th, 7th, 8th and 9th, the system only downloaded values equal to zero in the interval from 5:20 PM to 6:00 PM; on the 10th, 11th, 12th, 13th, 14th, 15th, 16th, 17th, 20th, 21st, 22nd, 24th, 25th, 26th, 27th, 28th, 29th, 30th and 31st the system only downloaded values equal to zero in the interval from 5:10:00 PM to 6:00:00 PM; on the 18th and 19th the system only downloaded values equal to zero in the interval from 5:00:00 PM to 6:00:00 PM; on the 23rd, the system only downloaded values equal to zero in the interval from 6:00:00 AM to 9:50:00 AM, but it did not download values for the rest of the day; in the month of June – on the 1st, 2nd, 3rd, 4th, 5th, 6th, 7th, 8th, 9th, 10th, 11th and 12th the system only downloaded values equal to zero in the interval from 17:10 PM to 06:00:00 PM hours; the system downloaded all data fluently from the 13th to the 30th of June in the

interval from 6:00:00 AM to 6:00:00 PM; in the month of July – on the 1st, 2nd, 3rd, 6th, 7th, 10th, 11th, 12th, 13th and 24th the system only downloaded values equal to zero in the interval from 06:00:00 AM to 06:10:00 AM and 5:10:00 PM to 6:00:00 PM; on the 4th, the system only downloaded values equal to zero in the interval from 6:00:00 AM to 6:10:00 AM and 5:00:00 PM to 6:00:00 PM; on the 5th, 8th and 9th, the system only downloaded values equal to zero in the interval from 6:00:00 AM to 6:20:00 AM and 5:10:00 PM to 6:00 PM;
On the 14th, 15th, 16th, 18th, 19th, 20th, 22nd, 26th, 27th, 28th, 29th, 30th and 31st the system only downloaded values equal to zero in the interval from 06:00:00 AM to 06:10:00 AM hours and 5:20:00 PM to 6:00:00 PM; on the 21st, the system only downloaded values equal to zero in the interval from 6:00:00 AM to 6:20:00 AM and 5:20:00 PM to 6:00:00 PM; on the 25th, the system only downloaded values equal to zero in the interval from 6:00:00 AM to 6:10:00 AM and 5:30:00 PM to 6:00:00 PM; in the month of August – on the 1st, 9th, 12th and 16th the system only downloaded values equal to zero in the interval from 5:20:00 PM to 6:00:00 PM; on the 2nd, 3rd, 5th and 9th, the system only downloaded values equal to zero in the interval from 6:00:00 AM to 6:10:00 AM and 5:20:00 PM to 6:00 :00 PM; on the 4th, 6th, 7th, 8th, 13th, 14th, 17th, 18th, 20th, 21st, 22nd, 23rd, 24th, 25th, 26th, 27th, 28th, 29th, 30th and 31st the system only downloaded values equal to zero in the interval from 5:30:00 PM to 6:00:00 P M;
On the 10th, 11th and 15th the system only downloaded values equal to zero in the interval from 6:00:00 AM to 6:10:00 AM and 5:30:00 PM to 6:00:00 PM; in the month of September – on the 1st, 3rd, 4th, 5th, 10th, 28th and 30th the system only downloaded values equal to zero in the interval from 5:30:00 PM to 6:00:00 PM; on the 2nd, 6th, 7th, 8th, 9th, 11th, 12th, 13th, 15th, 16th, 17th, 18th, 19th, 20th, 23rd, 24th, 25th, 26th and 27th the system only downloaded values equal to zero in the interval from 5:40:00 PM to 6:00:00 PM; on the 21st and 22nd the system only downloaded values equal to zero in the interval from 5:00:00 PM to 6:00 :00 M; on the 29th, the system only downloaded values equal to zero in the interval from 5:10:00 PM to 6:00:00 PM; in the month of October – on the 1st, 2nd, 3rd, 4th, 5th, 6th, 7th, 8th, 9th, 10th, 13th, 14th, 22nd and 23rd thе system only downloaded values equal to zero in the interval from 17:40:00 PM at 6:00:00 PM; on the 11th, 12th, 15th, 16th, 17th, 18th, 19th, 20th, 21st, 24th, 26th, 27th, 28th, 29th and 30th the system only downloaded values equal to zero in the interval from 5:50:00 PM to 6:00:00 PM hours; on the 25th and 31st, the system fluently downloaded all data in the interval from 6:00:00 AM to 6:00:00 PM;
In November – on the 1st, 2nd, 8th and 10th the system only downloaded values equal to zero in the interval from 5:50:00 PM to 6:00:00 PM; on days 3rd, 4th, 6th, 7th, 9th, 11th, 12th, 13th, 14th, 16th, 17th, 18th, 20th, 22nd, 23rd, 24th, 25th, 26th, 27th, 28th, 29th and 30th the system fluently downloaded all the data in the interval from 06:00:00 AM to 06:00:00 PM; on the 21st, the system only downloaded values equal to zero in the interval from 5:30:00 PM to 6:00:00 PM; and December – during all days of the month, the system fluently downloaded all data (interval from 06:00:00 AM to 18:00:00 PM).

Year 2014

January – during all days of the year (1st to 31st), the system downloaded all data fluently (interval from 6:00:00 AM to 6:00:00 PM); in February – during all days of the year (1st to 28th), the system fluently downloaded all data (interval from 6:00:00 AM to 6:00:00 PM); in the month of March – on the 1st, 3rd, 4th, 5th, 6th, 7th, 8th, 9th, 10th, 11th, 12th, 13th, 14th, 15th and 16th the system fluently downloaded all data in the interval from 06:00:00 AM to 06:00:00 PM hours; on the 2nd, 17th, 19th, 20th, 21st, 22nd, 23rd, 24th, 25th, 26th, 27th, 28th and 30th the system only downloaded values equal to zero in the interval from 5:50:00 PM to 6:00:00 PM hours; on the 29th and 31st the system only downloaded values equal to zero in the interval from 5:40:00 PM to 6:00:00 PM; in the month of April – on the 1st, 2nd, 3rd, 4th, 5th, 15th and 17th the system fluently downloaded all data in the interval from 5:40:00 PM to 6:00:00 PM;
During the 6th, 7th, 25th, 26th, 27th, 28th, 29th and 30th the system downloaded all data fluently (interval from 6:00:00 AM to 6:00:00 PM); on the 14th, the system only downloaded values equal to zero in the interval from 5:50:00 PM to 6:00:00 PM; on the 16th, 18th, 19th, 20th and 21st the system only downloaded values equal to zero in the interval from 5:30 PM to 6:00:00 PM; on the 22nd and 23rd the system only downloaded values equal to zero in the interval from 5:20:00 PM to 6:00:00 PM; on the 24th, the system only downloaded values equal to zero in the interval from 5:20:00 PM to 5:40:00 PM and from 5:50:00 PM to 6:00 PM; in the month of May – on the 1st, 28th and 29th, the system fluently downloaded all data in the interval from 06:00:00 AM to 06:00:00 PM;
On day 2nd, the system only downloaded values equal to zero in the interval from 5:40:00 PM to 6:00:00 PM; on the 3rd, 4th, 5th, 7th, 9th and 31st the system only downloaded values equal to zero in the interval from 5:10 PM to 6:00 PM; on the 6th, 8th, 10th, 11th, 12th, 13th, 14th, 15th, 16th, 17th, 18th, 19th, 20th, 21st, 22nd, 23rd, 24th, 25th and 26th the system only downloaded values equal to zero in the interval from 5:10:00 PM to 6:00:00 PM; on the 27th and 30th the system only downloaded values equal to zero in the interval from 6:00:00 AM to 6:10:00 AM; in the month of June – on the 1st and 2nd the system only downloaded values equal to zero in the interval from 6:00:00 AM to 6:10:00 AM and from 5:20:00 PM to 6:00:00 PM;
On the 3rd, 4th, 6th, 8th, 9th, 10th, 11th, 13th, 14th, 15th, 16th, 17th, 18th, 19th, 20th, 21st, 22nd, 24th, 25th and 27th the system only downloaded values equal to zero in the break from 6:00:00 AM to 6:10:00 AM and from 5:00:00 PM to 6:00:00 PM; on the 5th, 7th and 12th the system only downloaded values equal to zero in the interval from 6:00:00 AM to 6:10:00 AM and from 5:00:00 PM to 6:00:00 PM; in the month of July – on the 1st, 2nd, 3rd, 5th, 6th, 9th, 10th, 11th, 14th and 15th the system only downloaded values equal to zero in the interval from 06:00:00 AM to 06:10:00 AM and from

5:10:00 PM to 6:00:00 PM; on the 7th and 29th, the system only downloaded values equal to zero in the interval from 6:00:00 AM to 6:20:00 AM and from 5:10:00 PM to 6:00:00 PM; on the 8th, the system only downloaded values equal to zero in the interval from 5:00:00 PM to 6:00:00 PM; on the 17th, 18th, 19th, 20th, 21st, 22nd, 23rd, 24th, 25th, 27th, 28th, 30th and 31st the system only downloaded values equal to zero in the interval from 06:00:00 AM to 06:10:00 AM hours and from 5:20:00 PM to 6:00:00 PM; on the 26th,

The system only downloaded values equal to zero in the interval from 6:00:00 AM to 6:10:00 AM and from 5:20:00 PM to 6:00:00 PM; in the month of August – on the 11th, the system only downloaded values equal to zero in the interval from 5:10:00 PM to 6:00:00 PM; on the 2nd, 4th, 5th, 6th, 10th, 12th and 22nd the system only downloaded values equal to zero in the interval from 5:20:00 PM to 6:00:00 PM; on days 1st, 3rd, 7th, 8th, 9th, 13th, 14th, 15th, 16th, 17th, 18th, 19th, 20th, 21st, 23rd, 24th, 25th, 26th, 27th, 28th, 29th, 30th and 31st the system went down only values equal to zero in the interval from 5:30:00 PM to 6:00:00 PM; in the month of September – on the 1st, 2nd, 3rd, 4th, 5th, 6th, 12th and 19th the system only downloaded values equal to zero in the interval from 5:40:00 PM to 6:00:00 PM; on the 8th, 9th, 10th, 11th, 13th, 14th, 15th, 17th, 18th, 22nd, 23rd, 24th, 25th, 26th, 27th, 28th, 29th and 30th the system only lowered values equal to zero in the interval from 05:40:00 PM to 06:00:00 AM hours;

On the 20th and 21st the system only downloaded values equal to zero in the interval from 5:20:00 PM to 6:00:00 PM; in the month of October – on the 1st, 2nd, 3rd, 4th, 5th, 7th, 8th, 9th, 11th, 12th, 13th, 15th and 17th the system only downloaded values equal to zero in the interval from 5:40:00 PM to 06 :00:00 PM hours; on the 10th and 11th the system only downloaded values equal to zero in the interval from 5:50:00 PM to 6:00:00 PM; on the 14th, 26th, 27th, 29th, 30th and 31st the system only downloaded values equal to zero in the interval from 5:50:00 PM to 6:00:00 PM;

On the 17th, 18th, 19th, 20th, 21st, 22nd, 23rd, 24th, 25th and 28th the system fluently downloaded all data in the interval from 6:00:00 AM to 6:00:00 PM; in the month of November – on the 1st, 2nd, 3rd, 5th, 6th, 7th, 8th, 9th, 10th, 11th, 12th, 13th, 14th, 15th, 17th, 18th, 19th, 20th, 21st, 22nd, 23rd, 24th, 25th, 26th, 27th, 28th, 29th and 30th the system fluently downloaded all data in the interval from 6:00:00 AM to 6:00:00 PM; on days 2nd and 4th, the system only downloaded values equal to zero in the interval from 5:50:00 PM to 6:00:00 PM;

On the 16th the system only downloaded values equal to zero in the interval from 5:40:00 PM to 6:00:00 PM and in the month of December – on the 1st, 2nd, 3rd, 4th, 5th, 6th, 7th, 8th, 9th, 10th, 11th, 12th, 13th, 14th, 15th, 16th, 17th, 18th, 19th, 20th, 21st, 22nd, 24th, 25th, 28th, 29th, 30th and 31st the system fluently downloaded all data in the range from 6:00:00 AM to 6:00:00 PM; on the 26th, the system only downloaded values equal to zero in the interval from 5:40:00 PM to 6:00:00 PM.

FUNAE–Maputo–Lagoon Phati Station

Of the three years of medication, there were components equal to zero in the years 2013 and 2014, for this reason only the year 2012 (six months) was analyzed, which was the year of the beginning of the FUNAE Campaign in Lagoon Phati, with the following fluctuations:

In the month of April – he was not recorded data on the initial days of measurement, respectively on the 17th and 18th from 6:10:00:00 AM to 06:00:00 PM, measurements are recorded from 05:00:00 PM to 05:30:00 PM, and values equal to zero from 05:00:00 PM to 05:10:00 PM and from 05:40:00 PM to 06:00:00 PM, on the 27th, 28th and 29th, the system lowered values equal to zero, in the interval from 05:30:00 PM to 06:00:00 PM; in the month of May – on the 1st, 12th and 28th, the system only downloaded values equal to zero in the interval from 05:30:00 PM to 06:00:00 PM; on the 2nd, 3rd, 5th, 6th, 7th, 8th, 9th, 10th, 11th, 14th, 16th, 17th, 18th and 19th the system only downloaded values equal to zero in the interval from 05:20:00 PM to 06:00:00 PM hours; on the 13th,

The system fluently downloaded all the data in the interval from 06:00:00 AM to 06:00:00 PM; on the 15th, 20th, 21st, 22nd, 23rd, 24th, 25th, 26th, 27th, 29th, 30th and 31st the system only downloaded values equal to zero in the interval from 05:10:00 PM to 06:00:00 PM; in the month of June – on the 6th, 8th, 9th, 17th, 18th, 21st, 22nd and 29th, the system fluently downloaded all data in the interval from 06:00:00 AM to 06:00:00 PM; on days 1st, 2nd, 3rd, 4th and 5th the system lowered values equal to zero in the interval from 06:00:00 AM to 06:10:00 AM and from 05:10:00 PM to 06:00:00 PM, on the 7th, the system lowered values equal to zero in the interval from 05:20:00 PM to 06:00:00 PM, on the 10th, 13th and 23rd the system lowered values equal to zero in the interval from 06:00:00 AM to 06:20:00 AM and from 05:20:00 PM to 06:00:00 PM, on the 11th, the system downloads values equal to zero in the interval from 06:00:00 AM to 06:20:00 AM and from 05:50:00 PM to 06:00:00 PM hours.

On the 12th, the system lowered values equal to zero in the interval from 06:00:00 AM to 06:10:00 AM, on the 15th, the system lowered values equal to zero in the interval from 06:00:00 AM to 06:10:00 AM and from 04:30:00 PM to 06:00:00 PM, on the 16th, the system lowered values equal to zero in the interval from 06:00:00 AM to 06:30:00 AM; on the 19th, the system recorded values for the period from 06:00:00 AM to 11:50:00 AM and did not record measurements in the interval from 11:00:00 AM to 6:00:00 PM, on the 20th.

The system lowered values equal to zero in the interval from 06:00:00 AM to 06:40:00 AM and from 05:40:00 PM to 06:00:00 PM, on the 24th and 30th, the system lowered values equal to zero in the interval from 06:00:00 AM to 06:40:00 AM, on the 25th, the system lowered values equal to zero in the interval from 06:00:00 AM to 06:40:00 AM and from 05:10:00 PM to 06:00:00 PM, on the 26th and 27th, the system lowered values equal to zero in the interval from 06:00:00 AM to 06:40:00 AM and from 05:10:00 PM to 06:00:00 PM, on the 28th, the

system lowered values equal to zero in the interval from 06:00:00 AM to 06:50:00 AM, in the month of July – on the 6th, 8th, 17th, 21st, 22nd, 24th and 29th the system fluently downloaded all data in the interval from 06:00:00 AM to 06:00:00 PM, on days 1st, 2nd, 3th, 4th and 5th the system lowered values equal to zero in the interval from 06:00:00 AM to 06:10:00 AM and from 05:10:00 PM to 06:00:00 PM, on the 7th, the system lowered values equal to zero in the interval from 05:20:00 PM to 06:00:00 PM, on the 9th, the system lowered values equal to zero in the interval from 06:00:00 AM to 06:10:00 AM, on the 10th, 12th and 13th the system lowered values equal to zero in the interval from 06:00:00 AM to 06:30:00 AM and from 05:20:00 PM to 06:00:00 PM; on the 11th, the system lowered values equal to zero in the interval from 06:00:00 AM to 06:30:00 AM and from 04:50:00 PM to 06:00:00 PM, on the 14th, the system lowered values equal to zero in the interval from 06:00:00 AM to 06:30:00 AM and from 04:50:00 PM to 06:00:00 PM;

On the 15th, the system lowered values equal to zero in the interval from 06:00:00 AM to 06:20:00 AM and from 04:30:00 PM to 06:00:00 PM, on the 16th, the system lowered values equal to zero in the interval from 06:00:00 AM to 06:30:00 AM, on the 19th, the system measured values from 06:00:00 AM to 12:00:00 PM and from 12:00:00 PM to 06:00:00 PM it was not registering the measurement of values; on the 20th and 25th, the system lowered values equal to zero in the interval from 06:00:00 AM to 06:40:00 AM and from 05:40:00 PM to 06:00:00 PM; on the 23rd, the system lowered values equal to zero in the interval from 06:00:00 AM to 06:10:00 AM and from 05:20:00 PM to 06:00:00 PM; on the 26th and 27th, the system lowered values equal to zero in the interval from 06:00:00 AM to 06:40:00 AM and from 05:10:00 PM to 06:00:00 PM.

On the 28th, the system lowered values equal to zero in the interval from 06:00:00 AM to 06:50:00 AM, on the 30th, the system lowered values equal to zero in the interval from 06:00:00 AM to 06:30:00 AM; in the month of August – on the 1st, 2nd, 3rd, 4th, 5th, 6th, 7th, 8th, 9th, 10th, 11th, 12th, 13th, 14th, 15th and 16th the system fluently downloaded all data in the interval from 06:00:00 AM to 06:00:00 PM hours; on the 17th, the system lowered constant values equal to 1250.7 in the interval from 07:10:00 AM to 06:00:00 PM; on the 18th, the system lowered constant values equal to 1250.7 in the interval from 06:40:00 AM to 05:20:00 PM; on the 19th, the system lowered constant values equal to 1250.7 in the interval from 06:30:00 AM to 04:20:00 PM and from 06:40:00 AM to 06:00:00 PM, on the 20th, the system lowered constant values equal to 1250.7 in the interval from 06:40:00 AM to 06:00:00 PM.

On the 21st, the system lowered constant values equal to 1250.7 in the interval from 06:30:00 AM to 06:00:00 PM, on the 22nd, the system lowered constant values equal to 1250.7 in the interval from 07:30:00 AM to 03:50:00 PM; on the 23rd, the system lowered constant values equal to 1250.7 in the interval from 06:40:00 AM to 03:10:00 PM; on the 24th, the system lowered constant values equal to 1250.7 in the interval from 06:40:00 AM to 03:10:00 PM; on the 25th, the system lowered constant values equal to 1250.7 in the interval from 06:40:00 AM to 05:40:00 PM; on the 26th, the system lowered constant values equal to 1250.7 in the interval from 09:30:00 AM to 02:10:00 PM, from 02:50:00 PM to 03:00:00 PM and from 04:00:00 PM at 04:50:00 PM.

On the 27th, the system dropped constant values equal to 1250.7 in the interval from 08:00:00 AM to 05:20:00 PM; on the 28th, the system lowered constant values equal to 1250.7 in the interval from 06:50:00 AM to 03:40:00 PM; on the 29th the system lowered constant values equal to 1250.7 in the interval from 06:50:00 AM to 03:20:00 PM; on the 30th, the system lowered constant values equal to 1250.7 in the interval from 06:50:00 AM to 03:30:00 PM and on the 31st, the system lowered constant values equal to 1250.7 in the interval from 06:40:00 AM to 03:40:00 PM hours and in September – during all days of the month, the system fluently downloaded all data (interval from 06:00:00 AM to 06:00:00 PM hours).

Clear Index Determination Procedure

After selecting the sample and choosing the spectrum of 10 acceptable days, that is, days when the GHI approaches the Total Theoretical Radiation (acceptable day), or days when the Total Theoretical Radiation is much smaller than the GHI (day not acceptable) an algorithm was developed that leads to the calculation of the clear sky index, described below. Based on the month and day of the year, the number of days n elapsed until the day and time of measurement made by the pyranometer was determined, using the formulas provided in Table 2.

Table 2: Daily averages and n values for each month (Duffie & Beckman, 1991; Iqbal, 1983)

Month	n for i-th day of the month	For the daily average of days of the month	
		Date	δ
January	i	17	-20.9
February	31+i	16	-13.0
March	59+i	16	-2.4
April	90+i	15	9.4
May	120+i	15	18.8
June	151+i	11	23.1
July	181+i	17	21.2

August	212+i	16	13.5
September	243+i	15	2.2
October	273+i	15	-9.6
November	304+i	14	-18.9
December	334+i	10	-23.0

First, the given declination in degrees equation (1) was calculated (Duffie & Beckman, 1991; Iqbal, 1983)

$$\delta = 23.45\, Sin\left(360\frac{284+n}{365}\right) \quad (1)$$

Here the number of days n for each type of month day of the year was determined from Table 2.

Knowing the solar constant G_{sc} and the latitude ϕ for the location of each station, the hour angle ω_s was determined by the equation (2) (Belúcio, *et al.*, 2014; Duffie & Beckman, 1991; Iqbal, 1983; Kumar, 2016)

$$Cos\,(\omega_s) = -\frac{Sin\,\phi Sin\,\delta}{Cos\,\phi Cos\,\delta} = -tan\,\phi\,tan\,\delta \quad (2)$$

For Vianello and Alves, 1991, considering the chronological time variable H, which varies from 0 to 24 hours (in degrees), the hour angle w_s, in the morning and ws<0; at noon w_s=0 and in the afternoon ws>0, such that, after calculating the hour angle, taking into account the time (local time converted to solar). Having first, treating the measurement hour with a time interval of 1 (one) and 10 (ten) minutes, that is, minute by minute, then transforming the hour angle into degrees, a worse result was obtained equation (3). (Belúcio, *et al.*, 2014; Duffie & Beckman, 1991; Cumbane, 1994)

$\omega s=(H-12)\times 15$ (3)

The difference in minutes between solar time and standard time is (Duffie & Beckman, 1991; Iqbal, 1983; Mucomole *et al.*, 2021).

Tempo Solar-Tempo Padrão=$4\times(L_{st.}-L_{loc.}+E$ (4)

where $L_{st.}$ is the Standard Meridian for the local time zone; $L_{loc.}$ is the Longitude of the location in question, it is the Longitude in degrees east, which varies from $0<L<360^{\circ}$. Parameter E is the Equation of Time (given in minutes). (Duffie & Beckman, 1991; Iqbal, 1983; Mucomole *et al.*, 2021; Kumar, 2016)

$E=229.2\times(0.000075+0.001868\times CosB-0.032077\times SinB-0.014615\times Cos(2\times B)-0.04089\times Sin(2\times B))$ (5)

where B is given as, (Duffie & Beckman, 1991; Iqbal, 1983; Mucomole *et al.*, 2021)

$$B = (n-1)\times\frac{360}{365} \quad (6)$$

which ranges from $1\leq n\leq 365$.

Then, the zenith angle θ_Z, was found, using the equation (7),

$Cos\,\theta_Z = Cos\,(\phi)\,Cos\,(\delta)\,Cos\,(\omega s) + Sin\,(\phi)\,Sin\,(\delta)$ (7)

such that doing the inverse of the cosine, the respective zenith angle θ_Z was found, written in the equation (8),

$\theta_Z = Cos(Cos\,(\phi)\,Cos\,(\delta)\,Cos\,(\omega s) + Sin\,(\phi)\,Sin\,(\delta))$ (8)

The (averages of) the measured experimental radiation components were taken, and the extraterrestrial radiation on a horizontal surface can be calculated from the solar constant (incident energy in one hour), using the equation (9).

$$G_0 = G_{on} = G_{sc}\left(1+0.033Cos\,\frac{360n}{365}\right)Cos\,\theta_z \quad (9)$$

For horizontal surfaces, at any time between sunrise and sunset, the horizontal radiation can be defined by the equation (10).

$$G_0 = G_{on} = G_{sc}\left(1+0.033\,Cos\,\frac{360n}{365}\right)(Cos\phi Cos\delta Cos\,\omega_s + Sin\phi Sin\delta) \quad (10)$$

Then, an estimate of the clear sky radiation was made to know the level of absence of cloud dynamics in the sky, and the hypothetical particles that interfere with the mobility and arrival of solar radiation on the surface of the horizontal. The constants a_0, a_1 and k were determined for a standard atmosphere at 23 km visibility and found a_0^*, a_1^* and k^* which is given for altitudes lower than 2.5 km using the formulas (11), (12) and (13) (Duffie & Beckman, 1991; Iqbal, 1983; Mucomole *et al.*, 2021)

$a_0^*=0.4237-0.00821(6-A)^2$ (11)

$a_1^*=0.5055+0.00595(6.5-A)^2$ (12)

$k^*=0.2711+0.01858(2.5-A)^2$ (13)

and then the correction factors $r_0=a_0/(a_0^*)$, $r_1=a_1/(a_1^*)$ and $r_k=k/k^*$ were determined; that allowed, to calculate the atmospheric transmittance for the incident radiation τ_b, given by equation (14).

$G_{cnb}=G_{on}\,\tau_b$ (14)

where G_{on} is the extraterrestrial radiation incident on a plane normal to radiation on the same day and is expressed by: (Duffie & Beckman, 1991; Mucomole *et al.*, 2021)

$$G_{on} = \begin{cases} G_{sc}\left(1+0.0033\,\text{Cos}\,\dfrac{360n}{365}\right) & (15) \\ G_{sc}\left(1.000110+0.034221\,\text{Cos}\,B+0.001280\,\text{Sin}\,B \right. \\ \left. +0.000719\,\text{Cos}\,2B+0.000077\,\text{Sin}\,2B\right) \end{cases}$$

For the zenith angle, at an altitude above 2.5 km, the clear-sky normal DNI was calculated using equation (16) (Iqbal, 1983; Duffie & Beckman, 1991; Mucomole *et al.*, 2021)

$G_{cb}=G_{on}\,\tau_b\,Cos\theta_z$ (16)

and for periods of any hour, horizontal direct radiation was estimated using the formula (eq.17).

$I_{cb}=I_{on}\,\tau_b\,Cos\theta_z$ (17)

The diffuse radiation of the clear sky on a horizontal surface was determined to obtain the Total Theoretical Radiation, according to an empirical relation between the transmission coefficients developed by Liu and Jordan, (1960), through equation (18). (Duffie & Beckman, 1991; Liu & Jordan, 1960; Mucomole *et al.*, 2021)

$$\tau_d = \frac{G_d}{G_0} = 0.271 - 0.294\tau_b$$

where τ_d is $\frac{G_d}{G_0}$ (or $\frac{I_d}{I_0}$) is the ratio of DHI to extraterrestrial

DHI in the horizontal plane. (Belúcio, *et al.*, 2014; Duffie & Beckman, 1991; Liu & Jordan, 1960; Iqbal, 1983; Mucomole *et al.*, 2021)

$$K_t = \frac{GHI}{G_0}$$

The Total Theoretical Radiation was determined G_{Clear}= Total, which represents the sum between the direct radiation on the horizontal surface that arrives in a time given by the formula (16) and the diffuse radiation on the horizontal surface.

To remove the variability due to the reduction of incoming solar radiation on the horizontal surface, we introduce a normalized quantity, the brightness index, K_t (GHI ratio for daily extraterrestrial radiation) given as (Belúcio, *et al.*, 2014; Duffie & Beckman, 1991; Lohmann, 2018; Mills, 2011; Perez *et al.*, 2016),

$$K_t^* = \frac{GHI}{G_{Clear}}$$

or the clear-sky index K_t^* (ratio of GHI and clear-sky radiation, that is, the irradiation of the earth's atmosphere with clear-sky), the latter more effectively removing the effects of solar geometry in elevations and has a more intuitive range, and for good estimation, it has values ranging from 0 and not exceeding 1.4 (Duffie & Beckman, 1991; Lohmann, 2018 ; Perez *et al.*, 2016).

Where G_{Clear}= Total is the total radiation on the horizontal surface, that is, the sum between the direct radiation on the horizontal surface that arrives in a time given by the formula (16) and the diffuse radiation on the horizontal surface.

A time interval ΔK_t^* (variation between two consecutive measurements) of one and ten minutes was adopted, and the amplitude or period (interval of measurement of solar radiation on the horizontal surface) of one day (Devore, 2015; Mills, 2011; Perez *et al.*, 2016).

$$\Delta Kt^* = K(t+1)^* - Kt^* \quad (21)$$

Taking the ramp rate ΔK_t^* (variations of ΔK_t^*, for a period t) as dimensionable, the nominal variability (standard deviation of K_t^* and ΔK_t^*) or the index of the dimensional K_t^*, is (Belúcio, *et al.*, 2014; Devore, 2015; Duffie & Beckman, 1991; Lohmann, 2018; Mills, 2011).

$$\text{Nominal Variability} = \sigma(\Delta K_t^*) = \sqrt{(\text{var}[\Delta K_{t\,\Delta t}^*])} \quad (22)$$

The GHI and Total Theoretical Radiation spectra were used as a function of time to choose a maximum of 10 days with GHI behavior close to Total Theoretical Radiation, that is, acceptable for each month of the year 2012. The chosen days of each month were organized in a set that represents the whole year of 2012, in a table that contains the reference of the day, the average value of K_t^* and finally σK_t^*. Next, the spectrum of K_t^* was graphed as a function of ΔK_t^*, and the average value of K_t^* and the average value of ΔK_t^* were calculated.

On the basis of the graphs, the days were classified as cloudy, clear and intermediate skies, respectively. By convention it was defined that the days of the year, whose horizontal and vertical coordinates are located in the interval before the average of K_t^* and below σK_t^* as cloudy-sky days; the values whose coordinates are located in the interval after the average of the values of K_t^* and below σK_t^* were defined as clear sky days; and finally, the days whose coordinates are located above the σK_t^* values, regardless of what the K_t^* values are, were defined as intermediate-sky days.

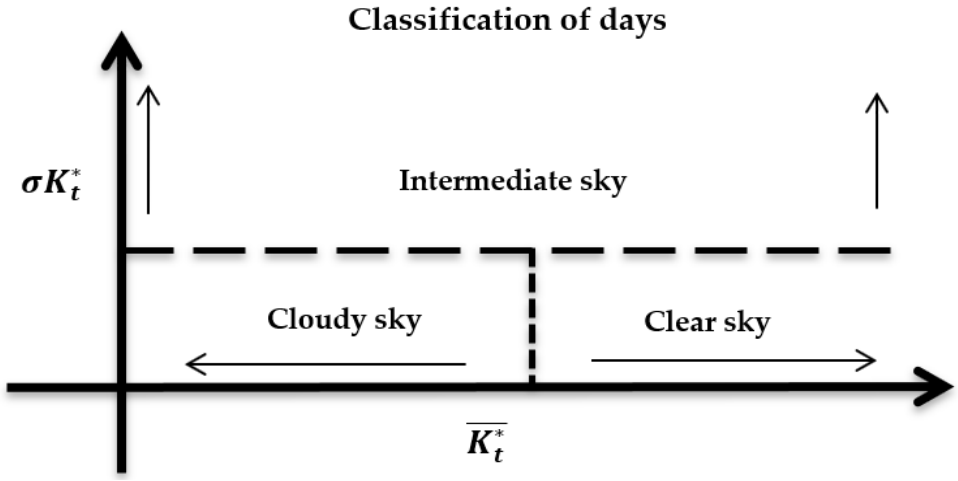

Figure 4: Classification of the days of each month of the year, using average values of K_t^* andσK_t^*.

After classifying the days, three days of different classifications were taken, and the spectrum of K_t^* and σK_t^* was trafficked as a function of the time of day, which allowed evaluating how solar energy varies throughout the day. Clear, cloudy and intermediate days were collected and counted, and new spectra were treated and constructed in a bar graph for analysis of the month of the year with the highest peak of cloudiness and clear days. ΔK_t^* Values were collected for each classification of days. Then, frequency density histograms were constructed to represent the spectrum of ΔK_t^*, for the three types of days. From these histograms, the variability of the selected days was analyzed for each day of the chosen year.

RESULTS

Classification of the days of the year

UEM–Maputo station

Year 2012

The calculation of the means values of K_t^* and σK_t^* for the year 2012 were equal to 0.8927 and 0.4650, using these values the diagram was obtained (see Figure 5).

From the spectrum obtained, it can clearly be concluded that all the days that are in the interval to the left of (K_t^*) =0.8927 and below σK_t^*=0.4650, represent the cloudy sky day and those that are to the right of (K_t^*) =0.8927 and below σK_t^*=0.4650, represent Clear Sky days, those that are in the interval above σK_t^*=0.4650 regardless of the values of (K_t^*), represents the days of intermediate sky.

It appears that during the 6 months analyzed: February, March, June, July, November and December, they present a layout that covers all seasons of the year. However, the following was observed: February has eight clear sky days, two cloudy sky days, and no intermediate sky days; The month of March has three days of clear skies, but has six days of cloudy skies and one day of intermediate skies, on the contrary; The month of June has a day with clear and cloudy skies, and also has an intermediate sky day; The month of July has one day of clear skies, four days of cloudy skies and three days of intermediate skies; The month of November has three days of clear skies, two days of cloudy skies and four days of intermediate skies, however; The month of December has five clear sky days, two intermediate sky days and three cloudy sky days, as shown in Table 3.

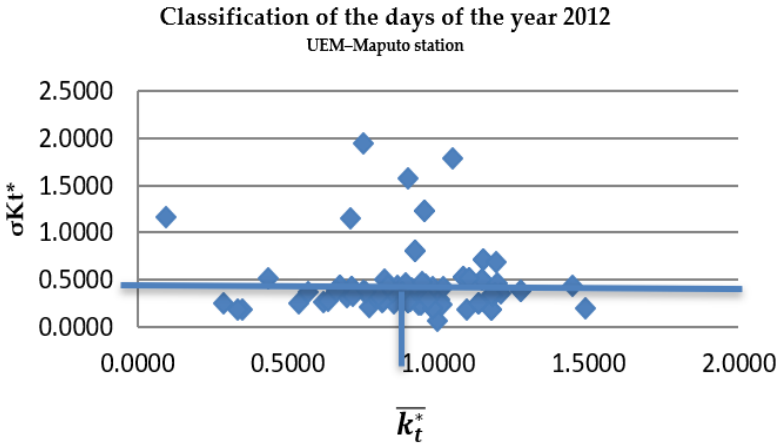

Figure 5: Scatter diagram for classifying the days of all months of the year 2012 in UEM–Maputo station, using the values of (K_t^*) and σK_t^* for each day.

Table 3: Distribution of the number of clear, cloudy and intermediate sky days in 2012.

Months	Classification		
	Clear	Cloudys	Intermediate
February	8	2	0
March	3	6	1
June	1	1	1
Jully	1	4	3
November	3	2	4
December	5	3	2
TOTAL	**21**	**18**	**11**

FUNAE–Gaza–Dindiza station

Year 2012

The calculations of the mean values of K_t^* and σK_t^* for the year 2012 were equal to 0.6594 and 0.2730, using these values the diagram was obtained (see Figure 6).

From the spectrum obtained, it can clearly be concluded that all the days that are in the interval to the left of (K_t^*)=0.6594 and below σK_t^*=0.2730, represent the cloudy sky day and those that are to the right of (K_t^*)=0.6594 and below σK_t^*=0.2730, represent Clear Sky days, those that are in the interval above σK_t^*=0.2730 regardless of whatever the values of (K_t^*), represents the days of intermediate sky. It appears that during the 9 months analyzed: April, May, December, July, June, August, September, October and November, they present a layout that covers all seasons of the year. However, the following was observed: The month of April does not have clear sky days, it has one cloudy sky day, and five intermediate sky days; The month of May does not have clear sky days, but has seven days of cloudy sky and one day of intermediate sky, on the contrary; The month of June does not have days of clear skies or intermediate

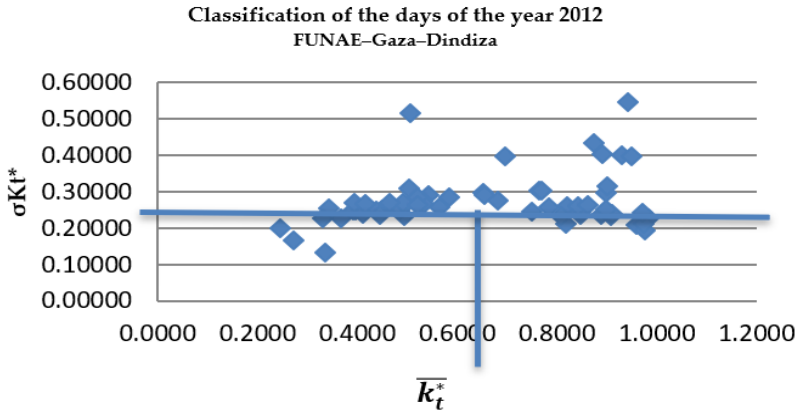

Figure 6: Scatter diagram for classifying the days of all months of the year 2012 in FUNAE–Gaza–Dindiza, using the values of K_t^* and σK_t^* for each day.

skies, but has six days of cloudy skies; The month of July does not have days of clear skies or intermediate skies, but has four days of cloudy skies; The month of August does not have days of clear skies or intermediate skies, but has two days of cloudy skies; September has two days of clear skies, three days of cloudy skies and one day of intermediate skies; The month of October has nine days of clear skies, does not have cloudy skies or intermediate skies; The month of November has nine days of clear sky, one day of cloudy sky and no days of intermediate sky, by the way; December has one clear sky day, nine intermediate sky days and no cloudy sky days, as shown in Table 4.

Table 4: Distribution of the number of clear, cloudy and intermediate sky days in 2012.

Months	**Classification**		
	Clear	**Cloudys**	**Intermediate**
April	0	1	5
May	0	7	1
June	0	6	0
July	0	4	0
August	0	2	0
September	2	3	1
October	9	0	0
November	9	1	0
December	1	0	9
TOTAL	**21**	**24**	**16**

Year 2013

The calculations of the means values of K_t^* and σK_t^* for the year 2013 were equal to 0.8646 and 0.3205, using these values the diagram was obtained (see Figure 8).

From the spectrum obtained, it can be clearly concluded that all the days that are in the interval to the left of K_t^* $\bar{}$=0.8646 and below σK_t^*=0.3205, represent the cloudy sky day and those that are right of K_t^* $\bar{}$=0.8646 and below σK_t^*=0.3205, represent Clear Sky days, those that are in the interval above σK_t^*=0.3205 regardless of what the

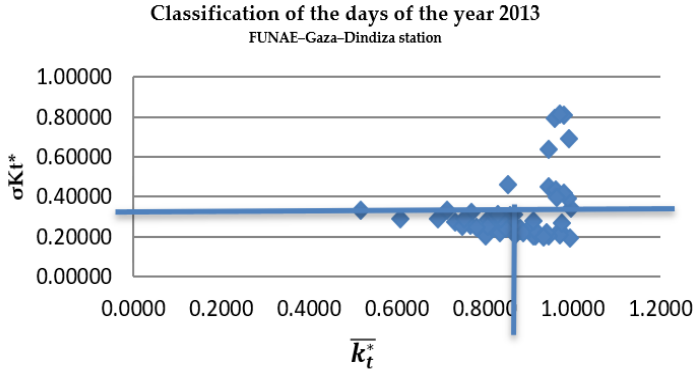

Figure 7: Scatter diagram for classifying the days of all months of the year 2013, using the values of Kt* $\bar{}$ and σK_t^* for each day.

values are of $K_t^{*\bar{}}$, represents the days of intermediate sky. It appears that during the 6 months analyzed: January, February, March, October, November and December, they present a layout that covers all seasons of the year. However, the following was observed: The month of January has a clear sky day, does not have cloudy sky days, and has nine intermediate sky days; February has two clear sky days, one cloudy sky day, and six intermediate sky days; The month of March has five days of clear skies, but five days of cloudy skies and no day of intermediate skies, on the contrary; The month of October, which has eight days of clear skies, but two days of cloudy skies and no day of intermediate skies, similarly; The month of November has eight days of clear skies, but two days of cloudy skies and no day of intermediate skies, however; The month of December has one clear sky day, two intermediate sky days and four cloudy sky days, as shown in Table 5.

Table 5: Distribution number of clear, cloudy and intermediate sky days in 2013.

Months	Classification		
	Clear	Cloudys	Intermediate
January	1	0	9
February	2	1	6
March	5	5	0
October	8	2	0
November	8	2	0
December	1	4	2
TOTAL	**25**	**14**	**17**

Year 2014

The calculations of the mean values of K_t^* and σK_t^* for the year 2014 were equal to 0.8459 and 0.3025, using these values the diagram was obtained (see Figure 8).

From the spectrum obtained, it can clearly be concluded that all the days that are in the interval to the left of $(K_t^*)^{\bar{}}$=0.8459 and below σK_t^*=0.3025, represent the cloudy sky day and those that are to the right of $(K_t^*)^{\bar{}}$=0.8459 and below σK_t^*=0.3025, represent Clear Sky days, those that are in the interval above σK_t^*=0.3025 regardless of whatever the values of $(K_t^*)^{\bar{}}$, represents the days of intermediate sky.

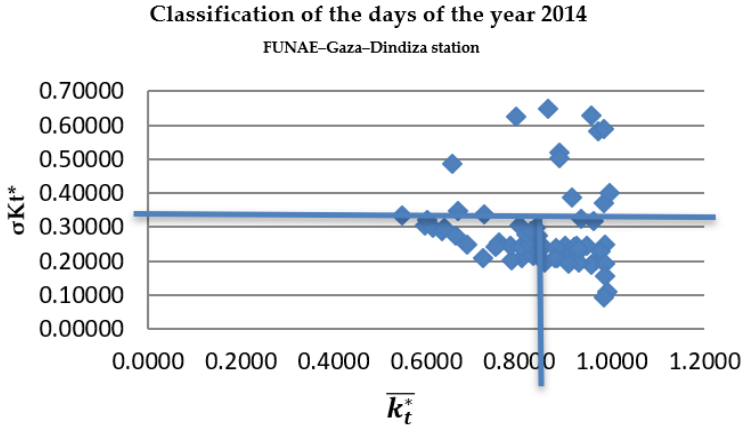

Figure 8: Scatter diagram for classifying the days of all months of the year 2014, using the values of $K_t^{*\bar{}}$ and σK_t^* for each day.

It appears that during the 8 months analyzed: January, February, March, April, September, October, November and December, they present a layout that covers all seasons of the year. However, the following was observed: The month of January has one clear sky day, no cloudy sky day, and nine intermediate sky days; February has two clear sky days, one cloudy sky day, and seven intermediate sky days; The month of March has three days of clear skies, but has six days of cloudy skies and one day of intermediate skies, on the contrary; The month of April has no clear sky day or intermediate sky days, and has three days of cloudy skies; The month of September does not have clear sky days or intermediate sky days, but has four days of cloudy skies; The month of October has seven clear sky days, three cloudy sky days, and no intermediate sky days; The month of November has seven days of clear sky, three days of cloudy sky and no day of intermediate sky, however; The month of December has three clear sky days, no cloudy sky days and six intermediate sky days, as shown in Table 6.

Table 6: Distributions of the number of clear, cloudy and intermediate sky days in 2014.

Months	Classification		
	Clear	Cloudys	Intermediate
January	1	0	9
Februuary	2	1	7
March	3	6	1
April	0	3	0
September	0	4	0
October	7	3	0
November	7	3	0
December	3	0	6
TOTAL	23	20	23

FUNAE–Maputo–Lagoa Phati station

Year 2012

The calculation of the mean values of Kt* and σKt* for the year 2012 were equal to 0.7403 and 0.5948, using these values the diagram was obtained (see Figure 9).

From the spectrum obtained, it can be clearly concluded that all the days that are in the interval to the left of K_t^{*} $^{-}$=0.7403 and below σK_t^{*}=0.5948, represent the Cloudy day and those that are to the right of K_t^{*} $^{-}$=0.7403 and below σK_t^{*}=0.5948, represent Clear Sky days, those that are in the interval above σK_t^{*}=0.3025 regardless of whatever the values of $(K_t^{*})^{-}$, represents the days of intermediate sky.

It appears that during the 6 months analyzed: April, May, June, July, August, September they present a layout that covers all seasons of the year. However, the following was

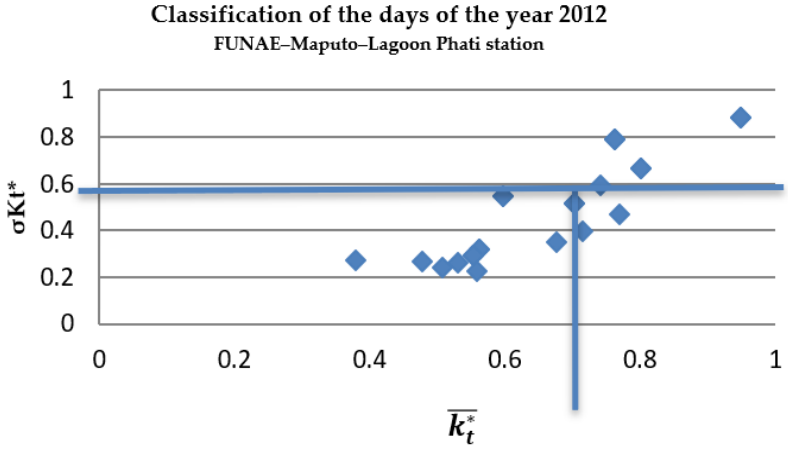

Figure 9: Scatter diagram for classifying the days of all months of the year 2012, using the values of Kt* $^{-}$ and σKt* for each day.

observed: The month of April, August and September had no one of the different skies days; the month of May has no clear sky days, one cloudy sky day, and no intermediate sky days; The month of June has one clear sky day, two days of cloudy skies and three days of intermediate skies, on the contrary; The month of July has no clear sky day but has four cloudy and intermediate skies days as shown in Table 7.

Table 7: Distributions of the number of clear, cloudy and intermediate sky days in 2012.

Months	Classification		
	Clear	Cloudys	Intermediate
April	0	0	0
May	0	1	0
June	1	2	3
July	0	4	4
August	0	0	0
September	0	0	0
TOTAL	**1**	**7**	**7**

Day Quantification Analysis

Clear, Cloudy and Intermediate sky day analysis chart

The final classification observed for the values of Table 3, 4, 5, 6, 7 and Figures 5, 6, 7, 8, 9 of the days shows that the six months of the year 2012 analyzed and calculated the values of K_t^* and σK_t^*, for the month of February presented a greater number of days of sky-clear about eight days and the month of June and July the least amount of clear sky days, about one day only. The month of March had the highest number of cloudy days, around six days, and the months of June and July had the lowest number of cloudy days each. The month of November registered the highest number of intermediate-sky days, about four days and the month of February did not record any intermediate-sky days, this behavior is applicable for the consider here regional stations in southern of Mozambique, as shown in the following figure,

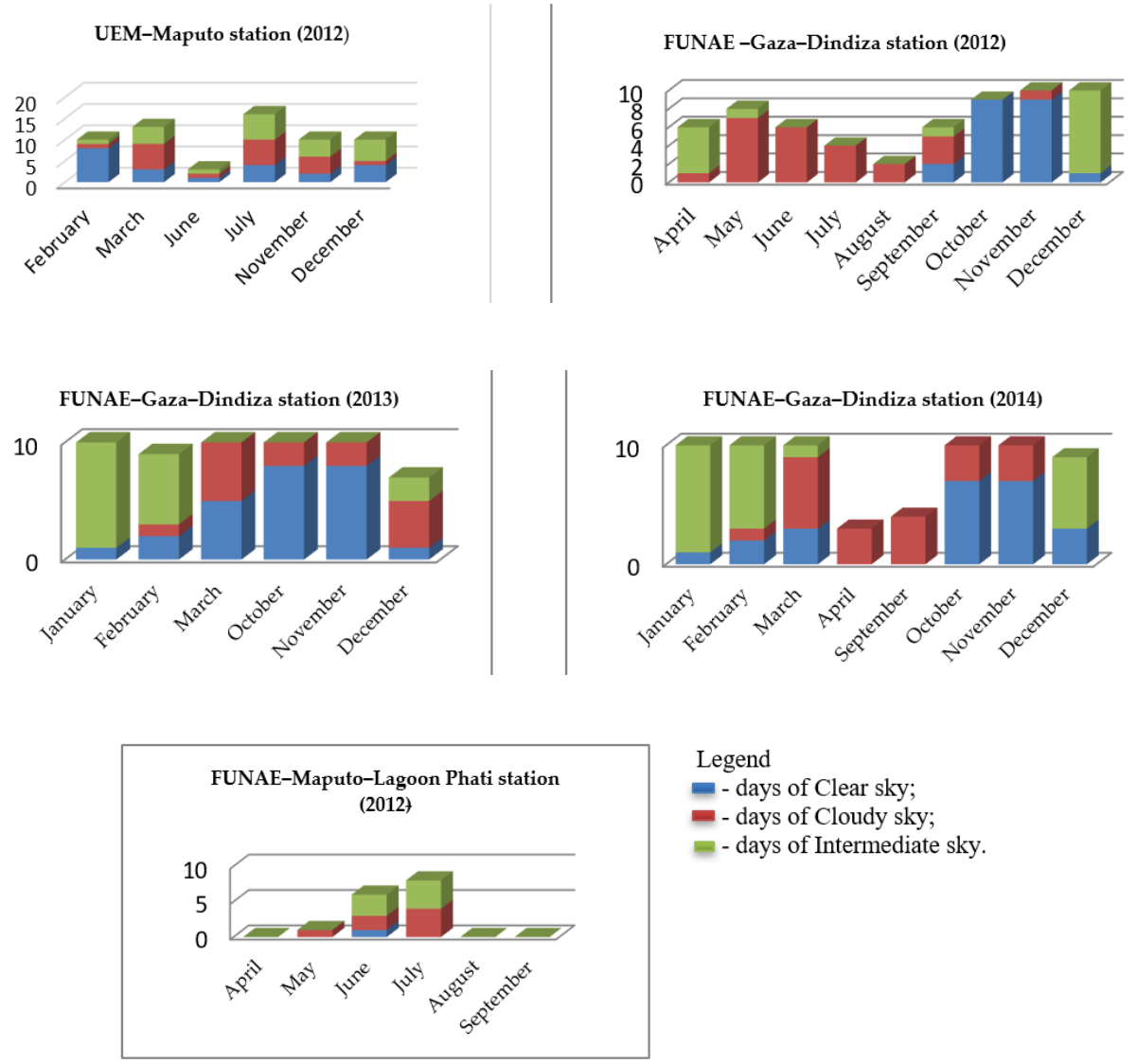

Figure 10: Temporal distribution diagram for classifying the days of the months, using the values of K_t^* and σK_t^* for each day of: (a) the year 2012, at the UEM–Maputo station; (b) the year 2012, at the FUNAE –Gaza–Dindiza station; (c) the year 2013, at the FUNAE–Gaza–Dindiza station; (d) the year 2014, at the FUNAE–Gaza–Dindiza station; (e) the year 2012, at the FUNAE–Maputo–Lagoon Phati station.

The rainy and hot season tends to have a higher relative percentage frequency of about 32.0 days with clear sky conditions, with a peak of greater frequency in the month of February at about 16.0, and the months of June and July with about 2.0 each. And a higher frequency of 12.0 days with intermediate sky conditions, with a peak in November at around 8.0. The dry and cold season tends to have a higher relative percentage frequency of about 22.0 days with a cloudy sky, with a peak of greater frequency in March of about 12.0.

Time Distribution for a Single Radiation Measurement Sensor

Clear Sky Day

The graph (in Figure11) clearly shows that from 6:00:00 AM solar radiation evolves until 8:00:00 AM and then

varies, registering sudden increases and decreases in the range of K_t^* values of 0.2 to 1.2 in the interval from 7:00:00 AM to 1:00:00 PM, then it varies slowly, and from 4:00:00 PM it starts to decrease, this smooth variation of Kt* and ΔK_t^*, relates to the weak cloudiness that the sky presents that does not impede the trajectory of solar radiation, based on the time interval of one minute.

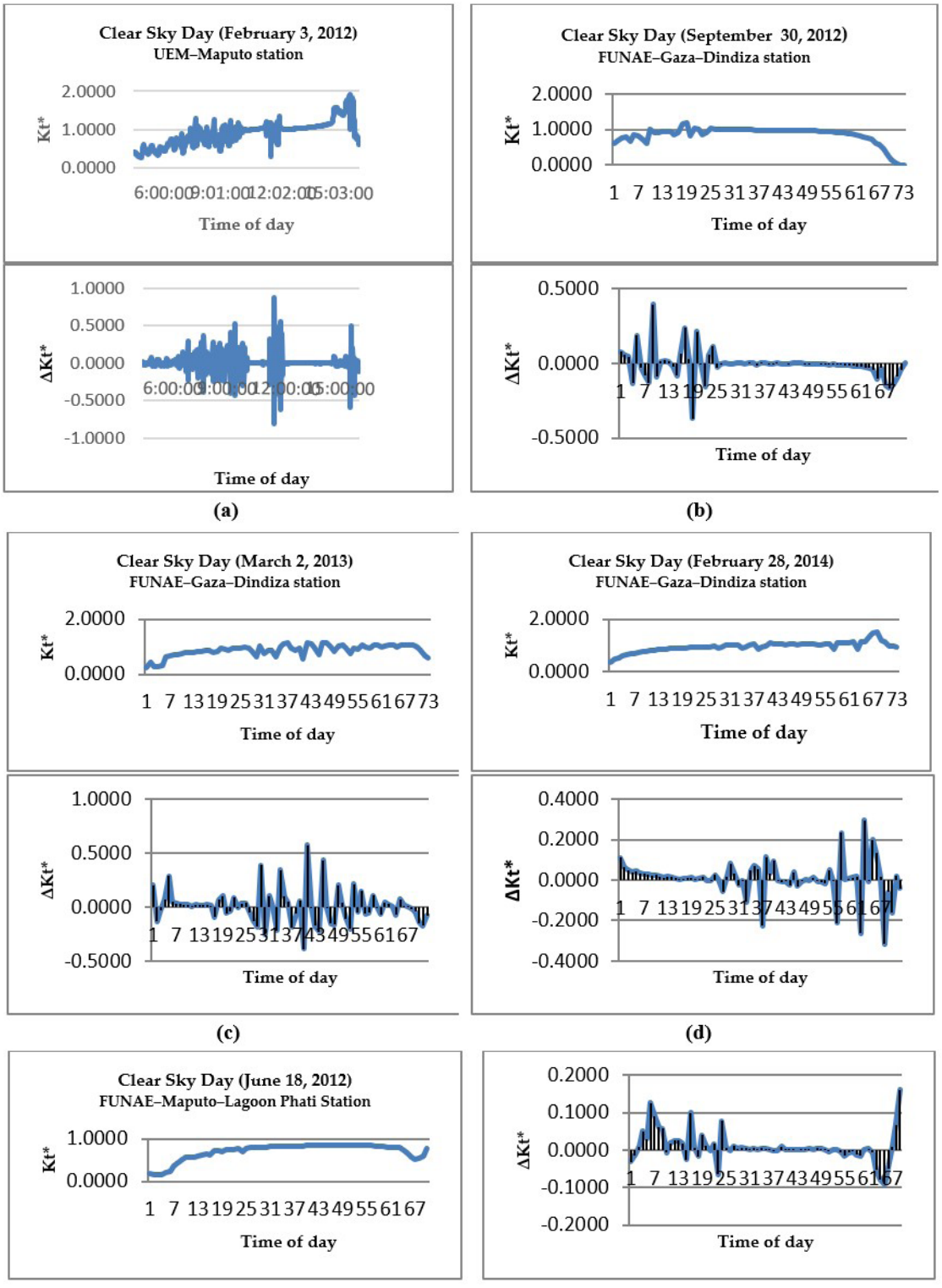

Figure 11: Distribution of K_t^* (top) and ΔK_t^* (bottom) as a function of time of day, (a) for a time interval of one minute and an amplitude of one day, over Clear Sky Day, February 3, 2012, at UEM–Maputo station; for a ten minute time interval and one day amplitude: (b) throughout clear day, September 30, 2012 , at FUNAE–Gaza–Dindiza station; (c) over clear day, March 2, 2013, at the FUNAE–Gaza–Dindiza station; (d) over clear day, February 28, 2014 , at the FUNAE–Gaza–Dindiza Station; (e) throughout clear day, February 28, 2012, at FUNAE–Maputo–Lagoon Phati Station.

Cloudy Sky Day

The spectrum (in Figure 12) clearly shows that from 8:00:00 AM to 3:00:00 PM, solar radiation varies abruptly, registering a complicated variation and then starts to increase from 5:00:00 PM , this is due to the strong amount of cloudiness observed in the order of 14.0 %, for a time interval of one and ten minutes.

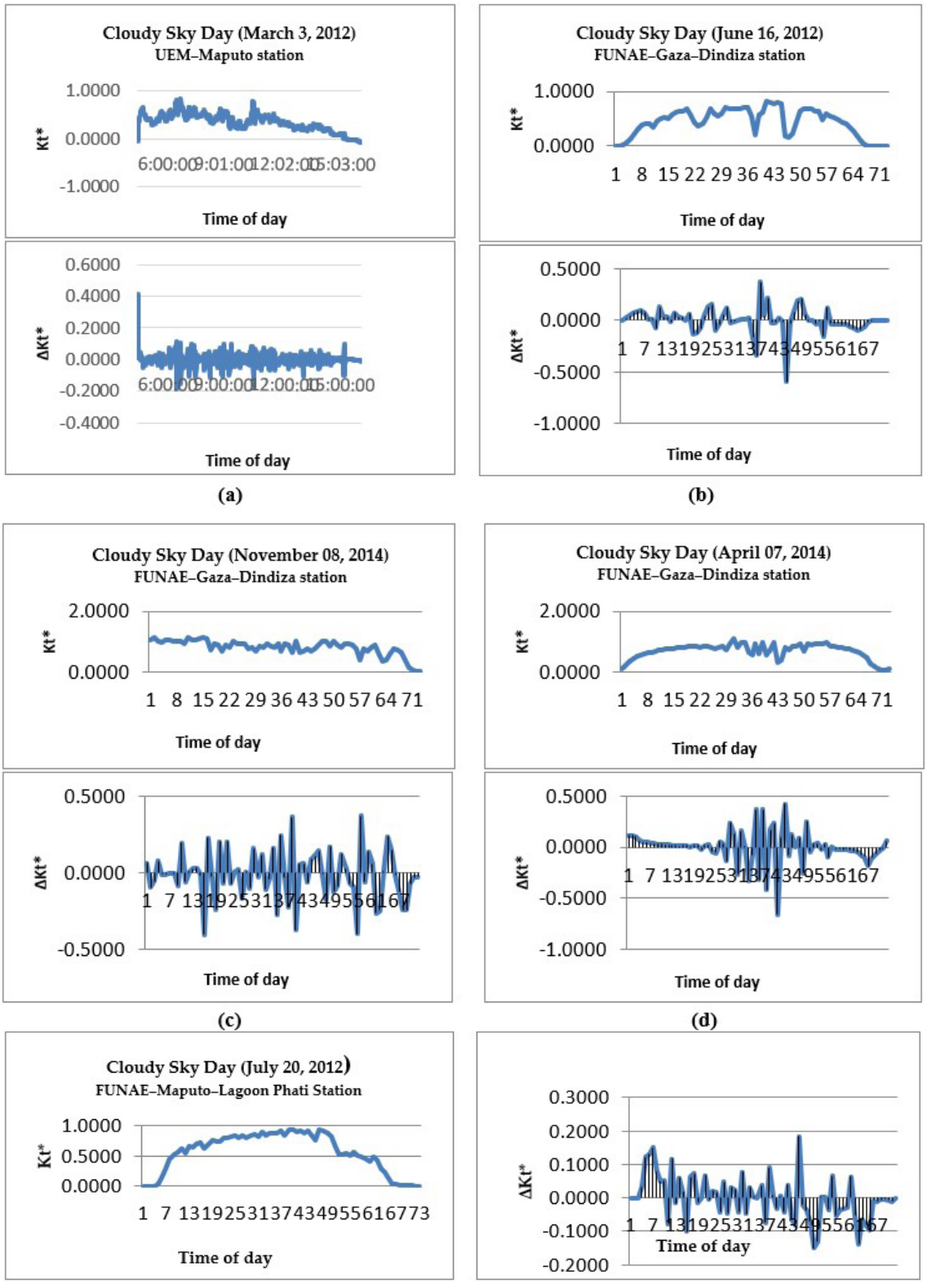

Figure 12: Distribution of K_t^* (top) and ΔK_t^* (bottom) as a function of time of day, (a) for a time interval of one minute and an amplitude of one day, over cloudy sky day, March 3, 2012, at UEM–Maputo station; for a ten minute time interval and one day amplitude: (b) throughout cloudy day, June 16, 2012, at FUNAE–Gaza–Dindiza station; (c) over cloudy day, November 08, 2014, at the FUNAE–Gaza–Dindiza station; (d) over cloudy day, April 07, 2014, at the FUNAE–Gaza–Dindiza Station; (e) throughout cloudy day, July 20, 2012, at FUNAE–Maputo–Lagoon Phati Station.

Intermediate-Sky Day

The spectrum (in Figure 13) shows a variation illustrating a sudden drop in solar radiation from 7:00:00 AM onwards due to the dynamics of cloud concentration at daybreak, causing K_t^* and ΔK_t^* remain in a decreasing direction; and the interval from 10:00:00 AM to 4:00:00 PM solar radiation shows a weak variability due to the fact that in this range there is little cloudiness also affecting the values of ΔK_t^* with the same behavior, then it decreases until the end of the day, because in this period we have cloud dynamics, based on a time interval of one and ten minute.

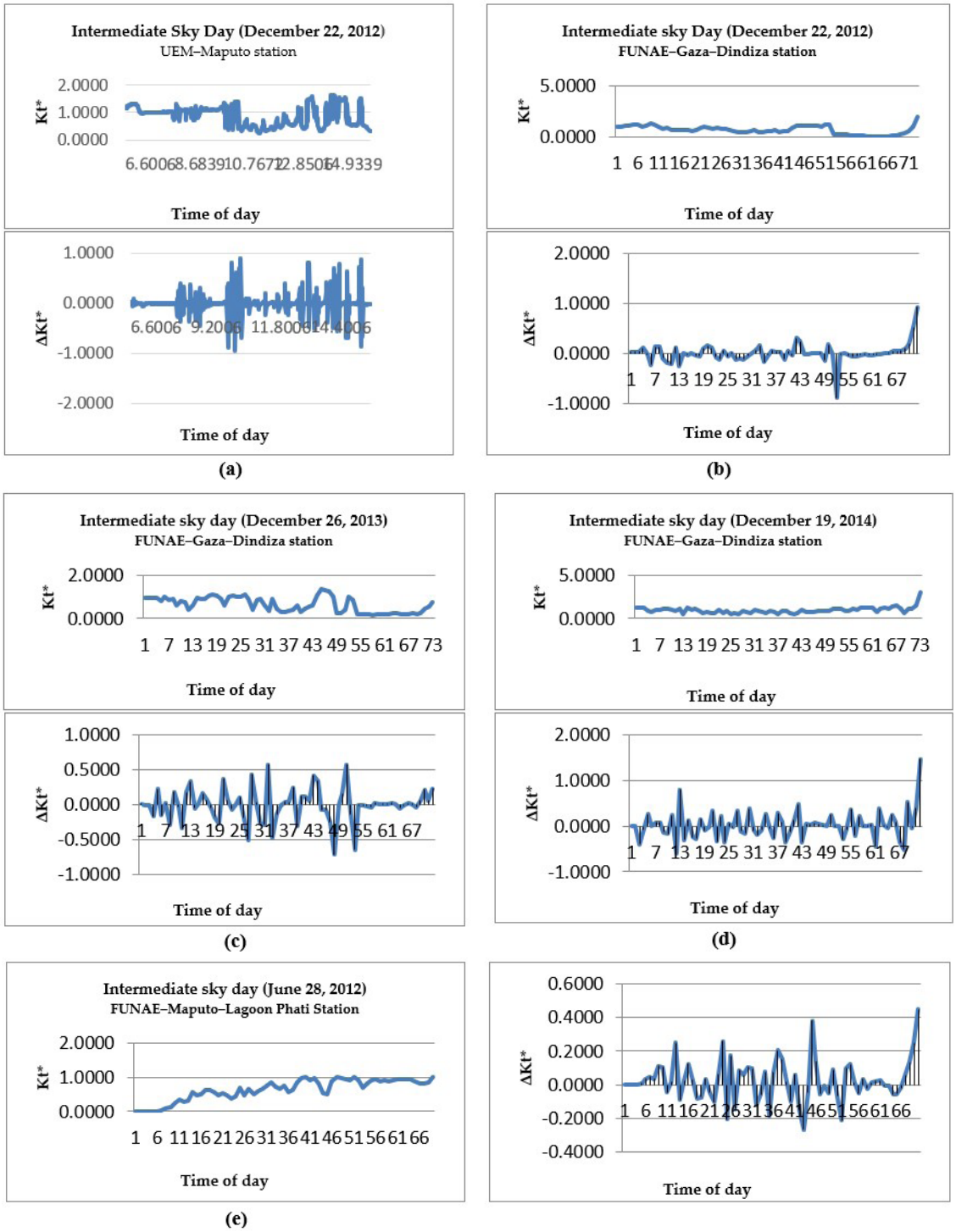

Figure 13: : Distribution of K_t^* (top) and ΔK_t^* (bottom) as a function of time of day, (a) for a time interval of one minute and an amplitude of one day, over intermediate sky day, December 22, 2012, at UEM–Maputo station; for a ten minute time interval and one day amplitude: (b) throughout intermediate day, December 22, 2012, at FUNAE–Gaza–Dindiza station; (c) over intermediate day, December 26, 2013, at the FUNAE–Gaza–Dindiza station; (d) over intermediate day, December 19, 2014, at the FUNAE–Gaza–Dindiza Station; (e) throughout intermediate day, June 28, 2012, at FUNAE–Maputo–Lagoon Phati Station.

It can be verified that the fluctuations during the daily course of the values of K_t^* determined according to its standard deviation for clear, cloudy and intermediate sky days,

It resembles the model adopted by Duffie & Beckman, (1991), for the calculation of global irradiation under clear sky (Figure 14), as an appropriate choice of time interval and amplitude for the study of variations.

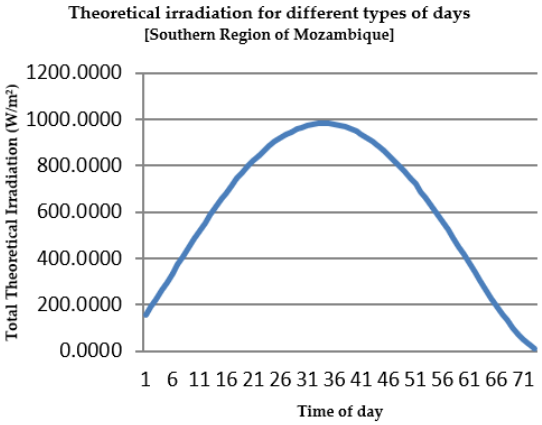

Figure 14: Total theoretical irradiation as a function of time of day.

Histograms of Clear, Cloudy and Intermediate days

The classification of data in Tables 3, 4, 5, 6 and 7, shows the separation of clear, cloudy and intermediate days, through which a new table can be built containing ΔK_t^* data for clear, cloudy and intermediate days of every year selected from the year, and resulted in histograms of variation of the probability density in the logarithmic scale, which will be analyzed below.

Variability of the clear sky index – K_t^* on a clear sky day

The frequency density has a maximum value for K_t^* close to zero, and gradually decreases as the K_t^* values increase in absolute value, reaching values lower than 0.03 when ΔK_t^* approaches 2.0.

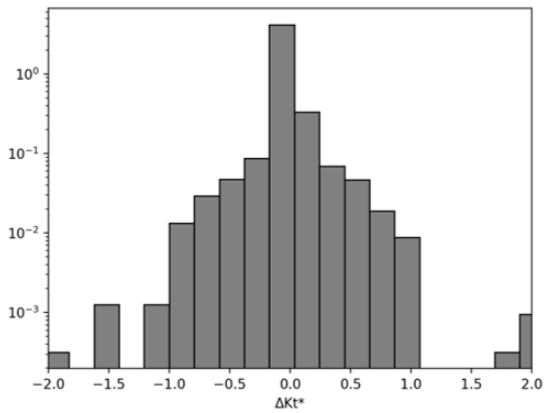

Figure 15: Distribution of variability on clear-sky days.

Variability of the clear-sky index – K_t^* on a Cloudy sky day

The cloudy sky days have the same behavior as the clear sky days described above, although when values lower than 0.03 are reached.

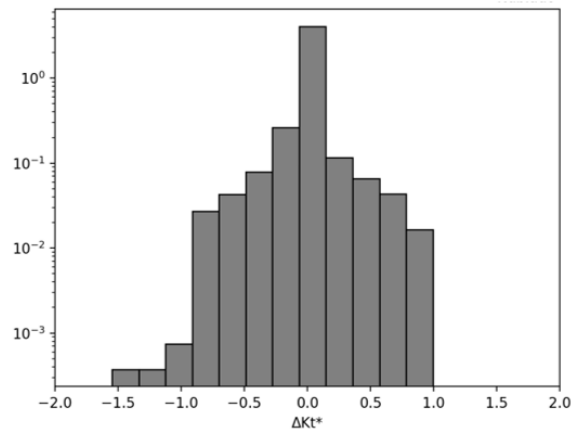

Figure 16: Distribution of variability on cloudy days.

Variability of the clear sky index – K_t^* on an intermediate sky day

The intermediate days also present a behavior similar to the previous ones, however the probability density presents a slight decrease, since the frequency of ΔK_t^* values in the interval outside [-2,2] is higher.

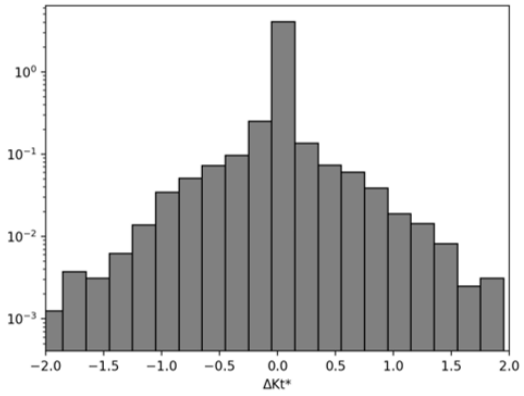

Figure 17: Distribution of variability on intermediate-sky days.

DISCUSSION

The mean values K_t^* and σK_t^* determined the interval for classifying the days as clear, cloudy and intermediate. Analyzing the southern region of Mozambique, in the sample of days of all stations, there is a trend of intermediate days in the percentage of: 22.0 0 % in the year 2012 in the UEM–Maputo station; in the FUNAE–Gaza–Dindiza station, 26.23 % in the year 2012, 32.69 % in the year 2013 and 34.85 % in the year 2014, at the FUNAE–Maputo–Lagoon Phati station 46.67 % in the year 2012. Cloudy days are in the percentage of: 36.0 % in the year 2012 at UEM–Maputo station; at FUNAE–Gaza–Dindiza station, 39.34 % in 2012, 19.23 % in 2013, 30.30 % in 2014; at FUNAE–Maputo–Lagoon Phati station, 46,67 % in the year 2012. And a higher percentage of the number of days are with clear skies, about: 42 % in the year 2012 at the UEM–Maputo station; at the FUNAE–Gaza–Dindiza station 34.43 % in the year 2012, 48.08 % in 2013 and 34.85 % in 2014; at the FUNAE–Maputo–Lagoon Phati station 46.6 7% in 2012. This classification took into account the evaluation of the dispersion diagram of the analyzed days of each month of the year previously mentioned (see Figures. 5, 6, 7, 8 and 9).

In the rainy and hot season (summer) where: in the UEM–Maputo station in the year 2012 there are a total of 29 days analyzed, it appears that about 32.0 % are in the clear sky condition, 14.0 % cloudy-sky days and 12.0 %, in the intermediate-sky condition; in the FUNAE–Gaza–Dindiza station in the year 2012 there are a total of 29 days analyzed, it appears that about 31.15 % are in the condition of clear sky, 1.64 % days of cloudy sky and 14.75 % in the intermediate sky condition; in the year 2013 there are a total of 46 days analyzed, it appears that about 35.71 % are in the clear sky condition, 16.07 % cloudy sky days and 30.36 % in the intermediate sky condition; in the year 2014 there are a total of 49 days analyzed, it appears that about 30.30 % are in the clear sky condition, 10.61 % cloudy sky days and 33.35 % in the intermediate sky condition; At the FUNAE–Maputo–Lagoon Phati station in the year 2012, there were no records of different days at this station due to the fact that this was the year in which the data reading began at this station and it did not include data reading failures by the logger, as previously mentioned.

On the other hand, in the cold and rainy season (winter): in the UEM–Maputo season in 2012, with a total of 21 days, 10.0 % have clear sky days, 22.0 % cloudy sky days and 10.0 % intermediate sky days; in the FUNAE–Gaza–Dindiza station in 2012, with a total of 32 days, 3.28 % had clear sky days, 37.70 % cloudy sky days and 11.48 % intermediate sky days; in 2013, with a total of 10 days, 8.93 % had clear sky days, 8.93 % cloudy sky days and 0.0 % intermediate sky days; in 2014, with a total of 21.0 days, 4.55 % had clear sky days, 9.09 % cloudy sky days and 1.52 % intermediate sky days; In the FUNAE–Maputo–Lagoa Phati station in 2012, with a total of 15.0 days, 6.67 % had clear sky days, 46.67 % cloudy sky days and 46.67 % intermediate sky days.

These results differ from those obtained by Fernando *et al.*, (2018). This difference may be related to the fact that this author regularly includes all days of the year in the sample, while this research evaluates only a small part of the sample. On the other hand Fernando *et al.*, (2018) base his analysis on the calculation of the daily solar energy flux.

Figure 11, which show the variation of the clear-sky index, for a time interval of one minute, registering a sudden increase and decrease in the range of K_t^* values from 0.2 to 1.2 from 6:00:00 AM solar radiation evolves until 7:00:00 AM and then varies sharply in the interval from 7:00:00 AM to 1:00:00 PM, then it varies slowly, from 4:00:00 PM onwards it begins to register a reduction. This smooth variation of K_t^* is related to weak cloudiness (adapted from Lohmann *et al.*, 2018).

On the other hand, Figure 12 shows the characteristic curve of a cloudy day. They show that for a time interval of one minute, from 8:00:00 AM to 3:00:00 PM, solar radiation varies sharply. This variation must be the strong amount of cloudiness observed.

The characteristic intermediate-sky curve shown in Figure 13, shows a slight increase in an interval of about half an hour (06:00:00 AM to 06:30:00 AM), then varies sharply due to concentration dynamics of cloudiness. These results are in agreement with the results presented during the shadow effect, there is a substantial significant reduction in variability.

The histograms showed in Figures 15, 16 and 17 shows the variability of σK_t^* for clear, cloudy and intermediate sky days, respectively. The decrease from the central peak of the frequency density shown in the histograms is smoother on intermediate sky days. This result reflects the greater variability on intermediate sky days.

CONCLUSION

The analysis of the results allows concluded the following: At the UEM–Maputo station, the density of analyzed values for the six months of the year 2012 shows that the values of K_t^* for one day vary between 0.3342–1.2764, with the minimum observed in July and the maximum in December. At the FUNAE–Gaza–Dindiza station, the density of analyzed values: of the nine months of the year 2012, shows that the values of K_t^* for one day vary between 0.2459 - 0.9832, with the minimum observed in month of June and the maximum in November; of the nine months of the year 2013, it shows that the values of K_t^* for a day vary between 0.4984–0.9961, with the minimum observed in January and the maximum in February; of the nine months of the year 2014, shows that the values of K_t^* for a day vary between 0.5483–0.9956, with the minimum observed in January and the maximum in February. At the FUNAE–Gaza–Lagoon Phati station, the density of analyzed values: of the nine months of the year 2012, shows that the values of K_t^* for one day vary between 0.5306–0.948, the minimum is observed in the month of May and the maximum in July.

In the UEM–Maputo station, in the year 2012, of the total of 50 days it can be seen that: 21 days have clear skies, 18 days have cloudy skies and 11 days have intermediate skies. At the FUNAE–Gaza–Dindiza station, during the year 2012, out of the total of 61 days it can be seen that: 21 days have clear skies, 24 days have cloudy skies and 16 days have intermediate skies; during the year 2013, of the total of 56 days it can be seen that: 25 days have clear skies, 14 days of cloudy skies and 17 days of intermediate skies; during the year 2014, of the total of 66 days it is verified that: 23 days have clear skies, 20 days of cloudy skies and 23 days of intermediate skies. And at the FUNAE–Maputo–Lagoon Phati station, during the year 2012, of the total of 15 days it can be seen that: 01 day has clear skies, 07 days of cloudy skies and 07 days of intermediate skies.

The variations during the daily course of K_t^* determined according to its standard deviation show as much adequacy to the model adopted for the calculation of the global irradiation in clear sky, as an appropriate election of the time interval and of the amplitude and of the period for the study of the variations.

The frequency with which higher absolute values of ΔK_t^* are presented is higher on intermediate-sky days.

Acknowledgment

Special thanks to the Mozambican agencies in the FUNAE, INAM and UEM entities that formally made available the data that supported the experimental testing of this scientific article, to the corresponding author upon reasonable request, and to NOAA, through which the data present in the platform were extracted http://www.ncdc.noaa.gov/orders/isd/3072547975015dat.txt. Included in local data processing.

REFERENCES

Arias-Castro, E.; Kleissl, J. & Lave, M. (2014). A Poisson model for anisotropic solar ramp rate correlations, *Sol. Energy, 101,* 182–200. https://doi.org/10.1016/j.solener.2013.12.028

Barreto, E. J. F. & Pinho, J. T. (2008). Hybrid Systems, Energy Solutions for the Amazon; Ministry of Mines, 1st Edition, Brazil. https://www.mme.gov.br/luzparatodos/downloads/Solucoes_Energeticas_para_a_Amazonia_Hibrido.pdf

Belúcio, L. P., Silva, A. P. N. D., Souza, L. R., & Moura, G. B. D. A. (2014). Radiação solar global estimada a partir da insolação para Macapá (AP). *Revista Brasileira de Meteorologia, 29,* 494-504. https://doi.org/10.1590/0102-778620130079

Burilo, G. A.; Estefanel, V.; Heldwein, A. B.; Prestes, S.D. & Horn, J. F. C. (2012). Estimativa da Radiação Solar Global A partir dos Dados de Insolação, Para Santa Maria – RS, *Ciência Rural, 42,* 1563-1567, Brazil. https://doi.org/10.1590/S0103-84782012005000059

Cumbane, J. J. (1994). Estudo do Efeito de Temperatura no Rendimento das Células Solares, *Eduardo Mondlane University, 1,* 19-78, Mozambique. https://energypedia.info/images/0/0f/PT_temperatura_das_celulas_solares_Cumbane.pdf

Corel draw (2020). https://coreldraw.en.uptodown.com/windows

Calif, R.; Schmitt, F. G.; Huang, Y., & Soubdhan, T. (2013). Intermittency study of high frequency global solar radiation sequences under a tropical climate, *Sol. Energy, 98,* 249–366. https://doi.org/10.1016/j.solener.2013.09.018

Curtright, A. E. & Apt, J. (2018). The character of power output from utility-scale photovoltaic systems, *Prog. Photovoltaics, 16,* 239–259, https://doi.org/10.1002/pip.786

Devore, J. (2015). Probability and Statistics for Engineering and the Sciences, Brooks/Cole, Cengage Learning, Boston. https://faculty.ksu.edu.sa/sites/default/files/probability_and_statistics_for_engineering_and_the_sciences.pdf

Duffie, A. J. & Beckman, A. W. (1991). Solar Engineering of Thermal Processes, 2ª edition, *John Wiley and Sons INC, 1,* USA, New York. https://www.sku.ac.ir/Datafiles/BookLibrary/45/John%20A.%20Duffie,%20William%20A.%20Beckman(auth.)-Solar%20Engineering%20of%20Thermal%20Processes,%20Fourth%20Edition%20(2013).pdf

EP – Energy Pedia (2022). https://energypedia.info/wiki/Potencial_em_Energias_Renov%C3%A1veis

Elsinga, B. & van Sark, W. (2014). Spatial power fluctuation correlations in urban rooftop photovoltaic systems: Spatial power fluctuation correlations, *Prog. Photovoltaics, 23,* 1380–1400. https://doi.org/10.1002/pip.2539

Freitas, S. S. (2008). Dimensionamento de Sistemas Fotovoltaicos, Master Thesis. https://bibliotecadigital.ipb.pt/bitstream/10198/2098/1/Susana_Freitas_MEI_2008.pdf

Fernando, D. M. Z. (2018). Irradiação Solar Global para Cidade de Maputo - Moçambique: Evolução Temporal das Medidas, Estudo da Cobertura do Céu e Modelagem Estatística, Master Thesis, Botucatu, Brazil. https://repositorio.unesp.br/bitstream/handle/11449/180261/fernando_dmz_me_botfca.pdf?sequence=3&isAllowed=y

FUNAE (2012, 2013 e 2014). Solar radiation datta

Fernando, D. M. Z. (2018). Irradiação Solar Global para Cidade de Maputo - Moçambique: Evolução Temporal das Medidas e Modelagem Estatística, Botucatu, Brasil. https://revistas.fca.unesp.br/index.php/energia/article/view/EnergAgric.2019v34n1p82-93

FUNAE–National Fund of Energy, (2022). https://funae.co.mz/quem-somos/

Gallego, C., Costa, A., Cuerva, A., Landberg, L., Greaves, B., & Collins, J. (2013). A wavelet-based approach for large wind power ramp characterization: A wavelet-based approach for large wind power ramp characterisation, *Wind Energy, 16,* 236–274. https://doi.org/10.1002/we.550

Greenpro (2004). Energia Fotovoltaica - Manual

Sobre Tecnologia Projecto e Instalação de Sitemas Fotovoltaicos, European Union. https://onlinelibrary.wiley.com/doi/epdf/10.1002/we.550

Google Earth (2021). https://www.googleearth.com

Hottel, H.C. (1971). Solar Energy, A simple model, for estimating the transmittance for direct Solar radiation Thought Clear Atmosphere, USA, New York. https://www.osti.gov/biblio/7348362;

Hoff, T. E. & Perez, R. (2010). Quantifying PV power output variability, *Sol. Energy, 84,* 1744–1830. https://www.solaranywhere.com/wp-content/uploads/2021/07/081_QuantifyingPVPowerOutputVariability.pdf

Hoff, T. E. & Perez, R. (2012). Modeling PV fleet output variability, *Sol. Energy, 86,* 1000–2190, https://doi.org/10.1016/j.solener.2011.11.005

Hinkelman, L. M. (2013). Differences between along-wind and cross-wind solar irradiance variability on small spatial scales, *Sol. Energy, 88,* 189–303, https://doi.org/10.1016/j.solener.2012.11.011

Inman, R. H.; Pedro, H. T. C. & Coimbra, C. F. M. (2013). Solar forecasting methods for renewable energy integration, USA. https://doi.org/10.1016/j.pecs.2013.06.002

Izidine, P. (2008). Elaboração de um atlas de ventos para Moçambique usando o Modelo Regional do Clima RegCM, Eduardo Mondlane University, Department of Physics, Mozambique. http://monografias.uem.mz/bitstream/13456789/590/1/2008%20-%20Pinto%2C%20Izidine.pdf;

INAM. (2020, 2021 and 2022). Solar radiation datta – Traditional station.

INAM. (2020, 2021, 2022). Solar radiation datta – Automatic station (Davis Station).

Iqbal, M. (1983). An introduction to solar radiation, Academic Toronto. https://shop.elsevier.com/books/an-introduction-to-solar-radiation/iqbal/978-0-12-373750-2

Kumar, D. (2016). Sacramento Solar Variability, A Thesis Presented to Faculty of The Department of Mechanical Engineering, California State University Sacramento, Master of science in Mechanical Engineering, California, Sacramento (not published)

Klima, K. & Apt, J. (2015). Geographic smoothing of solar PV: results from Gujarat, Environ. *Res. Lett., 10,* 104001. https://doi.org/10.1088/1748-9326/10/10/104001

Lohmann, G.M.; Monahan, A.H. & Heinemann, D. (2016). Local short-term variability in solar irradiance, Atmos. *Chem. Phys. 16,* 6365–6379, Canada. https://doi.org/10.5194/acp-16-6365-2016

Lohmann, G. M. (2018). Irradiance Variability Quantification and Small-Scale Averaging in Space and Time: A Short Review, Energy Meteorology Group, Institute of Physics, June, Oldenburg University, Germany. https://doi.org/10.3390/atmos9070264

Liu, B. Y. H. & Jordan, R. C. (1960). Solar energy The Interrelationship and Characteristic Distribution of Direct and Total Solar Radiation, 4, USA, New York. https://doi.org/10.1016/0306-2619(87)90044-4

Lave, M. and Kleissl, J. (2010). Solar variability of four sites across the state of Colorado, *Renew. Energ., 35,* 2633–2944. https://doi.org/10.1016/j.renene.2010.05.013

Lave, M. & Kleissl, J. (2013). Cloud speed impact on solar variability scaling – Application to the wavelet variability model, *Sol. Energy, 91,* 10–19. https://doi.org/10.1063/5.0050428

Lave, M., Kleissl, J., & Arias-Castro, E. (2012). High-frequency irradiance fluctuations and geographic smoothing, *Sol. Energy, 86,* 2080–2233. https://doi.org/10.1016/j.solener.2011.06.031

Lave, M., Kleissl, J., & Stein, J. S. (2013). A Wavelet-Based Variability Model (WVM) for Solar PV Power Plants, *IEEE Transactions on Sustainable Energy, 4,* 411–612. https://doi.org/10.1109/TSTE.2012.2205716

Lonij, V. P., Brooks, A. E., Cronin, A. D., Leuthold, M., & Koch, K. (2013). Intra-hour forecasts of solar power production using measurements from a network of irradiance sensors, *Sol. Energy, 97,* 56–70. https://doi.org/10.1016/j.solener.2013.08.002

Luoma, J., Kleissl, J., & Murray, K. (2012). Optimal inverter sizing considering cloud enhancement, *Sol. Energy, 86,* 421–430. https://doi.org/10.1016/j.solener.2011.10.012

Madhavan, B. L., Kalisch, J., & Macke, A. (2016). Shortwave surface radiation network for observing small-scale cloud inhomogeneity fields, *Atmos. Meas. Tech., 9,* 1090–1200. https://doi.org/10.5194/amt-9-1153-2016

Marcos, J., Marroyo, L., Lorenzo, E., Alvira, D. & Izco, E. (2011). From irradiance to output power fluctuations: the PV plant as a low pass filter, *Prog. Photovoltaics, 19,* 415–600, 2011. https://onlinelibrary.wiley.com/doi/abs/10.1002/pip.1063

Marcos, J., Marroyo, L., Lorenzo, E., Alvira, D., & Izco, E. (2011). Power output fluctuations in large scale PV plants: One year observations with one second resolution and a derived analytic model, *Prog. Photovoltaics, 19,* 218–227. https://doi.org/10.1002/pip.1016

Mills, A. (2011). Implications of Wide-Area Geographic Diversity for Short-Term Variability of Solar Power, Lawrence Berkeley National Laboratory, Berkeley, California, USA. https://www.osti.gov/servlets/purl/986925

Macedo, Al. S. & Fisch, G. (2017). Variabilidade Temporal da Radiação Solar Durante o Experimento GOAmazon 2014/15, *Revista Brasileira de Meteorologia, 33(*1), 353-365, Brazil. https://doi.org/10.1590/0102-7786332017. Available online: https://www.scielo.br/j/rbmet/a/FXTDwZB6hWzgyJbRYdDBTbs/?lang=pt, accessed on May 01, 2021 at 18:25 PM

Melo, V. F. (2003). Estudo do Comportamento da Radiação Solar na Região Sul do Save, *Eduardo Mondlane University, 1*(1), Mozambique. https://energypedia.info/wiki/File:PT Estudo_do_comportamento_da_radiacao_solar_da_regiao_Sul_do_Save-Victor_

Fl%C3%A1vio_de_Melo.pdf

Mucomole, F. V., Dombo, C & Cuamba, B. C. (2013). Dimensionameto de Um sistema Fotovoltaico Para Fornecer Energia Eléctrica Numa Incubadora, Licenciate final work, Eduardo Mondlane University, Mozambique. https://pt.scribd.com/

Mucomole, F. V., Bnitez, E. R. V & Cuambe, V. A. (2021). Variabilidade temporal da disponibilidade da energia solar nas condições da Cidade de Maputo – caso do ano 2012, Master thesis, Eduardo Mondlane University, Mozambique

NOAA (2020, 2021 and 2022). Solar radiation datta. http://www.ncdc.noaa.gov/orders/isd/3072547975015dat.txt

Neggers, R. A. J., Jonker, H. J. J. & Siebesma, A. P. (2003). Size statistics of cumulus cloud populations in large-eddy simulations, *J. Atmos. Sci., 60,* 1050–1074.https://journals.ametsoc.org/view/journals/atsc/60/8/1520-0469_2003_60_1060_ssoccp_2.0.co_2.xml

Ohmura, A.; Gilgen, H.; Hegner, H.; Müller, G.; Wild, M. ; Dutton, E. G. ; Forgan, B.; Fröhlich, C.; Philipona, R.; Heimo, A.; König-Langlo, G.; McArthur, B.; Pinker, R.; Whitlock, C. H.; & Dehne, K.. (1998). Baseline Surface Radiation Network (BSRN/WCRP): New Precision Radiometry for Climate Research, *B. Am. Meteorol. Soc. 79,* 2115–2136. https://doi.org/10.1175/15200477(1998)079<2115:BSRNBW>2.0.CO;2

Perpiñán, O.; Marcos, J. & Lorenzo, E. (2009). Electrical power fluctuations in a network of DC/AC inverters in a large PV plant: Relationship between correlation, distance and time scale, *Sol. Energy, 88,* 227–241, 2-13. https://doi.org/10.1016/j.solener.2012.12.004

Piacentini, R. D.; Salum, G. M.; Fraidenraich, N. & Tiba, C. (2011). Extreme total solar irradiance due to cloud enhancement at sea level of the NE Atlantic coast of Brazil, *Renew. Energ., 36,* 409–412. https://doi.org/10.1016/j.renene.2010.06.009

Paint Net (2022). https://www.getpaint.net/download.html

Python 3.8.5 software (2020). https://python.en.uptodown.com/windows

Perez, R.; David, M., Hoff, T.; Kivalov, S.; Kleissl, J.; Lauret, P. & Perez, M. (2016). Spatial and Temporal Variability of Solar Energy, Foundations and Trens in Renewable Energy, USA, New York. https://doi.org/10.1561/2700000006

PER–Portal of Renewable Energies (2022). https://www.portal-energia.com/capacidade-solar-fotovoltaica-2050-148115/

Perez, R.; Kivalov, S.; Schlemmer, J.; Hemker Jr., K. & Hoff, T. E. (2012). Short-term irradiance variability: Preliminary estimation of station pair correlation as a function of distance, *Sol. Energy, 86,* 2170–2176. http://www.clca.columbia.edu/9_Perez_Solar_Variability.pdf

Stetz, T.; von Appen, J.; Niedermeyer, F.; Scheibner, G.; Sikora, R.; & Braun, M. (2015). Twilight of the Grids: The Impact of Distributed Solar on Germany's Energy Transition, *Power and Energy Magazine, IEEE, 13,* 50–61. https://doi.org/10.1109/MPE.2014.2379971

Suri, M.; Huld, T.; Dunlop, E.; Albuisson, M.; Lefevre, M. & Wald, L. (2007). Uncertainties in solar electricity yield prediction from fluctuation of solar radiation, 22nd European Photovoltaic Solar Energy Conference, September, Milan, Italy. https://publications.jrc.ec.europa.eu/repository/handle/JRC36426

Souza, M. J. H.; Ribeiro, A.; Leite, F. P. & Gois, G. (2005). Avaliação do Modelo de Bristow & Campbell na Estimativa, Média Mensal dos Totais Diários da Irradiação Solar Global Para o Vale do Rio Doce, MG. In: Congresso Brasileiro de Agrometeorologia, Anais., Campinas: SB. Agro, CD-ROM, Brazil, Campinas. http://sbagro.org/files/biblioteca/1645.pdf

Twidell, John & Weir, Tony (1996). Renewable Energy Resources, 3rd edition, E & FN SPON editor, *An Imprint of Chapman & Hall, 2,* USA, New York. https://doi.org/10.4324/9781315766416

UEM (2012). Solar radiation data (one minute temporal resolution)

Van Haaren, R.; Morjaria, M. & Fthenakis, V. (2018). Empirical assessment of short-term variability from utility-scale solar PV plants: Assessment of variability from utility-scale solar PV plants, *Prog. Photovoltaics, 22,* 548–559. https://doi.org/10.1002/pip.2302

Vianello, R. L. & Alves, A. R. (1991). Meteorologia Básica e Aplicações, Viçosa: UFV Imprensa Universitária, 300-410, Brasil. https://www.editoraufv.com.br/produto/meteorologia-basica-e-aplicacoes-2-edicao/1110587

Wenham, Stuart R.; Green, M.A; Watt, M.E. & Corkish, R. (2007). Applied Photovoltaics, Second Edition, Britsh library, Earthscan in the UK and USA. https://10.4324/9781849776981;

Yordanov, G.; Saetre, T. & Midtgard, O.-M. (2013). Optimal temporal resolution for detailed studies of cloud-enhanced sunlight (Overirradiance), Photovoltaic Specialists Conference (PVSC), IEEE 39th, 0985–0988. https://doi.org/10.1109/PVSC.2013.6744306,2013b

Yordanov, G.; Midtgård, O.-M.; Saetre, T.; Nielsen, H. & Norum, L. (2013). Overirradiance (Cloud Enhancement) Events at High Latitudes, *IEEE Journal of Photovoltaics, 3,* 271–277. https://10.1109/JPHOTOV.2012.2213581

Zekai, S. (2008). Solar Energy Fundamentals and Modeling Techniques, Atmosphere Environment Climate Change and Renewable Energy, London, England. https://download.e-bookshelf.de/download/0000/0078/33/L-G-0000007833-0002336688.pdf